JGR Oceans

RESEARCH ARTICLE
10.1029/2021JC017808

Persistent Ross Sea Freshening From Imbalance West Antarctic Ice Shelf Melting

S. S. Jacobs[1], C. F. Giulivi[1], and P. Dutrieux[1,2]

[1]Lamont-Doherty Earth Observatory of Columbia University, Palisades, NY, USA, [2]British Antarctic Survey, Cambridge, UK

Key Points:

- A 63-year Ross Sea salinity decline, overlain by variability tied to Amundsen Sea winds, parallels regional and global climate changes
- Net mass loss from SE Pacific ice shelves since 1970 is more than enough to account for observed freshening in the downstream Ross Sea
- Lower seawater density has not enhanced warm deep water access to the Ross continental shelf, but could end local Antarctic Bottom Water formation by 2060

Supporting Information:

Supporting Information may be found in the online version of this article.

Correspondence to:

S. S. Jacobs,
sjacobs@ldeo.columbia.edu

Citation:

Jacobs, S. S., Giulivi, C. F., & Dutrieux, P. (2022). Persistent Ross Sea freshening from imbalance West Antarctic ice shelf melting. *Journal of Geophysical Research: Oceans*, *127*, e2021JC017808. https://doi.org/10.1029/2021JC017808

Received 27 JUL 2021
Accepted 18 FEB 2022

Author Contributions:

Conceptualization: S. S. Jacobs
Data curation: S. S. Jacobs, C. F. Giulivi
Funding acquisition: S. S. Jacobs, P. Dutrieux
Investigation: S. S. Jacobs, C. F. Giulivi, P. Dutrieux
Methodology: S. S. Jacobs, C. F. Giulivi, P. Dutrieux
Project Administration: S. S. Jacobs
Resources: S. S. Jacobs, C. F. Giulivi, P. Dutrieux
Software: C. F. Giulivi
Supervision: S. S. Jacobs

Abstract A 63-year observational record in the southwest Ross Sea shows a continuing, near-linear salinity decrease of 0.170 and slight warming of 0.013°C through 2020. That freshening exceeded any increase in sea ice production and brine release from stronger southerly winds, while melting and freezing at the Ross Ice Shelf base contributed little to the salinity change. The parallel seawater density decline appears not to have enhanced warm deep water intrusions onto the continental shelf (CS). Confirming prior inferences, the salinity change has been mainly caused by a growing imbalance in the meltwater available from thinning ice shelves and increased iceberg calving in the upstream Amundsen and Bellingshausen Seas. Shorter-term salinity variability has tracked winds near the Amundsen Sea CS break, in turn coherent with a broader Pacific climate variability index, and with salinity reversals on and seaward of the Ross CS. The melt driven freshening is positively correlated with global atmospheric CO_2 and temperature increases, and adds to the rise in sea level from increased glacier flow into weakened ice shelves. Continued erosion of those ice shelves could end the production of high salinity shelf and bottom waters, as defined in the Ross Sea, by the 2050s.

Plain Language Summary Prior reports of salinity change in the Ross Sea have relied on selected observations over a limited area, and assumptions about a probable cause. In this study we documented freshening over 63 years, accompanied by slight warming, from measurements obtained during 43 summers in a wider region on the southwest Ross continental shelf. Minor net melting under the adjacent Ross Ice Shelf may have helped to offset additional brine release by sea ice formation under stronger surface winds. However, most of the freshening has resulted from an increasing volume of West Antarctic ice shelf and iceberg meltwater transported westward by coastal and slope currents. Seawater density is dominated by salinity at cold temperatures, parameters that began to reveal change ~50 years ago as a shifting atmospheric circulation increased "warm" deep water access to vulnerable ice shelves. Downstream freshening of the Ross Sea and its Antarctic Bottom Water then resulted from meltwater sources that have increased by more than 10 billion tons each year, a remote impact of anthropogenic climate change with regional to global effects on ocean properties and sea level.

1. Introduction and Acronyms

This study extends and strengthens earlier records of thermohaline change in the Ross Sea, and considers its forcing and implications. A key focus is the High Salinity Shelf Water (HSSW) that has long dominated the western continental shelf (CS), with salinities above ~34.6 (PSS-78) and near-freezing temperatures (Carmack, 1977; Jacobs et al., 1970; Orsi & Wiederwohl, 2009). By 2008 the salinity of post-International Geophysical Year (1957–1958) shelf water near Ross Island (RI, Figure 1) had declined by ~0.03/decade, while the upper 200 m of summer profiles near the CS break and central Ross Ice Shelf (RIS) had freshened by ~0.08/dec (Jacobs & Giulivi, 2010). We use decadal rates in figures; annual rates, often from cited material over shorter periods, also appear in the text. Dense shelf waters on Antarctic continental shelves, historically attributed to brine drainage from strong sea ice formation and export from coastal polynyas (Gill, 1973), are also influenced by precipitation, evaporation, the properties of seawater supply, and meltwater from sea ice, ice shelves and icebergs. Adding more freshwater (FW) or less salt lowers shelf water density, and subsequent mixing with deep and near-surface waters over the continental slope influences the salinity and volume of Antarctic Bottom Water (AABW; Purkey & Johnson, 2012). HSSW additionally fuels basal melting far beneath the RIS, reducing shelf water density and lowering its temperature to the pressure-dependent freezing point, followed by upwelling and basal freezing (Lewis & Perkin, 1986). The halosteric effect of freshening raises sea level beyond that caused by increased glacier flow into the ocean from excess ice shelf thinning (Munk, 2003; Rye et al., 2014).

Validation: S. S. Jacobs, C. F. Giulivi, P. Dutrieux
Visualization: C. F. Giulivi, P. Dutrieux
Writing – original draft: S. S. Jacobs
Writing – review & editing: S. S. Jacobs, C. F. Giulivi, P. Dutrieux

Temporal change in Ross Sea freshening (RSF) includes both decadal and shorter-term variability, such as a recent near-bottom salinity rebound northwest of RI in Terra Nova Bay (TNB), not caused by its persistent polynya (Castagno et al., 2019). That increase has been attributed to wind anomalies reducing the volume of sea ice imported onto the eastern CS (Comiso et al., 2011; Silvano et al., 2020). There is little evidence to suggest an increase in sea ice melting on the Ross CS, or in precipitation minus evaporation (Bromwich et al., 2011; Porter et al., 2019). Here we compile a longer, more detailed record of dense shelf water salinity near RI, considering its response to sea ice production and export, and to melting of the RIS by Antarctic Surface Water (AASW), HSSW and Modified Circumpolar Deep Water (MCDW). Quantified glacial meltwater volumes from upstream West Antarctic Ice Sheet (WAIS) sources are then paired with salinity change and residence time on the Ross CS to assess FW supply versus demand. Updated observations of abyssal thermohaline variability downstream of the CS follow RSF comparisons with regional and global rates of earth system change.

2. Data and Methods

Tracking of salinity and temperature change in the southwest Ross Sea was initially based on 200–800 m averages within ∼15 km of 77.167°S, 168.333°E, a site north of RI and directly downstream of the Ross Sea Polynya. Data from 500 m in McMurdo Sound was later added (Jacobs & Giulivi, 2010), showing little evidence of depth or spatial bias. Here we enhance and lengthen that sparse, 18-profile data set, using quality controlled measurements at 500 m from ships, ice holes and profiling drifters over a larger study area (Figure 1). That regional extent attempts to limit the influence of outflows containing basal meltwater (e.g., Robinson et al., 2010), while reaching beneath the McMurdo Ice Shelf and to a RIS cavity inflow region east of RI. Only summer (DJF) profiles are used, being the most commonly sampled. The 500 m depth is close to the CS average seaward of the RIS (Hayes & Davey, 1975; Timmermann et al., 2010), permitting the use of shallower profiles, and reducing noise from more variable conditions in the upper water column. Anticipating higher variability from single-depth values over a larger region, multiple observations from the same summer are averaged and equally weighted west and north of RI. The resulting "standard level" data set (Table S1 in Supporting Information S1) is based on 137 profiles from 1956 to 1957 through 2019–2020, 08 December–25 February, with four gaps of more than 2 years, the longest from 1984 to 1990.

Over the 6.3 decades covered by this study, instrumentation has evolved from individual sample bottles with mercury thermometers at discrete levels, closed by wire-sliding messengers, through continuous profiling with low accuracy "STD"s to higher precision conductivity-temperature-depth CTDs, to drifting profilers deployed from ships and aircraft. In the early 1980s reported ocean depth units changed from meters to decibars, but with 500 dbar ∼494 m and nearly isohaline profiles at depth, we use those units interchangeably. We have retained the PSS-78 salinity and in situ IPTS-68 temperature scales of most observations, noting that TEOS-10 absolute salinities are ∼0.18 higher at 500 m. Water samples processed on shipboard salinometers were typically calibrated with IAPSO standard seawater, although standard water batch numbers were not always reported, or post-cruise sensor recalibrations applied. The older bottle and STD salinity data are less accurate than the ±0.002 now achievable, but encompass an initial period of change, with +0.006/dec through 1969–1970 (Figure 2) becoming −0.010/dec through 1972–1973. Some observations suggest systematic offsets, largest in 1960–1961 when average ship-based 500 m salinities differed by 0.06 from average ice-hole observations that summer. Except for two 1960s stations, acceptable summer salinities lie within two standard deviations of a least squares regression, excluding the outliers shown and several other off-scale measurements. As oxygen isotope data in the Ross Sea are the subject of ongoing work, we only note here that samples near the RIS in 2007 (Friedrich & Schlosser, 2013) lengthen a late twentieth century drift suggestive of increasing glacial meltwater content (Jacobs et al., 2002).

Interpreting and modeling ocean change typically relies on climatologies based on past observations for reference, initialization and verification. Most historical ocean measurements near Antarctica have been acquired sporadically during austral summers, with dense shelf water properties taken to reflect winter forcing. Although moorings, drifting floats and instrumented seals are increasingly providing year-round and multi-year information, the resulting data can provide less accurate salinities and tend to be dispersed over various archives. An inventory of available Ross Sea station data through the early 2000s (Orsi & Wiederwohl, 2009), defined seasonal means, volumes and distributions within specified ranges. Shelf water salinities then ranged from 34.52 to 34.87 on the inner shelf, ∼93% saltier than an assigned HSSW threshold of 34.62. Only 63% exceeded that value in a 2007 section along the RIS, after which the 500 m salinity near RI decreased to a record minimum in

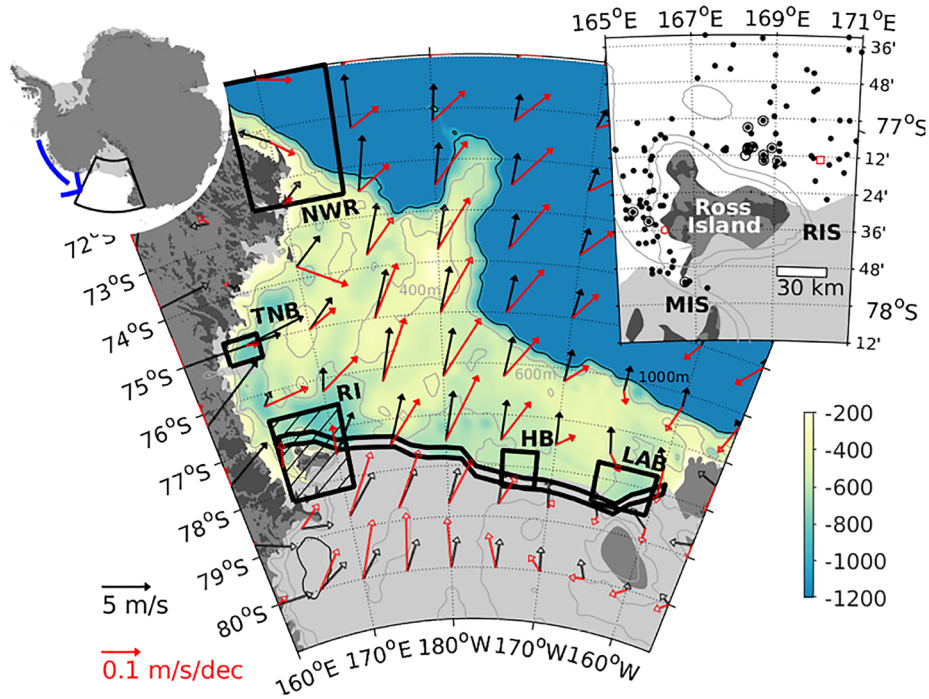

Figure 1. Ross Sea continental shelf (CS) bathymetry and the northern Ross Ice Shelf, with ERA5 average surface winds and trends, March-November, 1956–2019. Insets provide a circumpolar context for upstream inflow to the Ross CS, and show the Ross Island area, adjacent McMurdo Ice Shelf, and summer (DJF, 1956–1957 through 2019–2020) ocean stations used in Figures 2–4, 6, S1 and Tables S1 and S2 in Supporting Information S1. Circled profile sites were used in prior work; red circle/square sites are from 1911/1936. Winds over the CS area also appear in Figure 5. Other boxed areas locate Figure 4 observations in/near Terra Nova Bay, Hayes Bank and Little America Basin, and on the northwest Ross continental slope (Figure 8).

2014, and had risen sharply by 2016 (Castagno et al., 2019). In the interest of providing a continuous time series for comparative use, interpolation across data gaps in the 63 year, 500 m record near RI forms a potential RSF Index, with associated temperatures (Table S2 in Supporting Information S1), short-term variability and rising FW equivalent (Section 3.7).

3. Results

3.1. Salinity and Temperature Change on the Ross Sea Continental Shelf

Seawater properties on the Ross CS are influenced by sea ice formation and melting, changes in the atmosphere and ocean circulations, precipitation and evaporation, iceberg melting and by basal freezing and melting under floating glacial ice. The net result for 500 m salinity in HSSW near RI in summer (DJF) has been a change of −0.027/dec from 1956–1957 to 2019–2020 (Figure 2). That is essentially the same as a 1958–2008 estimate of −0.03/dec (Jacobs & Giulivi, 2010), rounded from −0.028/dec. The longer term near-linear decrease has been punctuated by excursions to higher and lower values, ranging from 34.93 in 1965 to 34.674 in 2014. No significant trend was apparent before the 1970s, but over the full record a linear regression drops below 34.8 in 1982, 34.7 in 2019, and its continuation would reach 34.6 in the 2050s. Most of an accompanying temperature trend of +0.002°C/dec is an effect of decreasing salinity on the surface freezing temperature. Decadal average salinity/depth profiles near RI in Figure 3 are bracketed by single station extremes in 1965 and 2014. Prior to 1956–1957, a 1936 profile with deep salinities similar to the 1970s is less stratified above 100 m, as is a shallow 1911 record. The latter salinities were “rather likely” biased high by difficult sampling conditions and processing after lengthy storage (Deacon, 1975), although subsequent freshening of 0.027/dec would have covered ∼70% of the distance from 1911 to the 1957–1969 mean profile. The decadal average profiles in Figure 3 show subsurface freshening near RI since the 1957–1969 period, during which any trend was negligible (Figure 2). The deep water column structure has been relatively stable over time, drifting toward lower values with a few spurious inversions

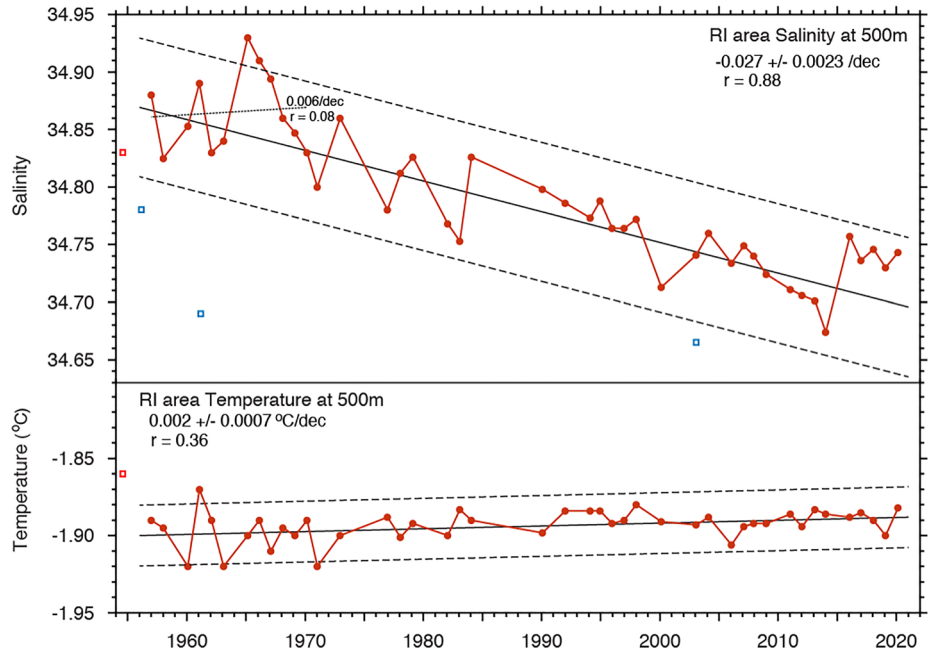

Figure 2. Summer (DJF) salinity and in situ temperature at 500 m near Ross Island (Figure 1) from single or averaged profiles in 43 years of a 63-year record (Tables S1 and S2 in Supporting Information S1). Solid linear regressions, bracketed by dashed lines at ±2 standard deviations, indicate net changes of −0.170 on the practical salinity scale and +0.013°C. The short dotted salinity regression applies to the period from 1956–1957 through 1969–1970. Boxes show realistic measurements in 1936 (red, at left) and some salinity outliers (blue).

resulting from averaging variable-depth salinity profiles. Salinities at 500 m from other circumpolar locations during the 1990s were similar on the southwest Ross and Weddell continental shelves, and have changed little in the Weddell since 1980 (Janout et al., 2021), suggesting different seawater supply or forcing in those comparable environments.

Earlier deep salinity records near the Ross Sea coastline, lengthened in Figure 4, are saltier westward under the influence of successive coastal leads and polynyas along the perimeter of generally clockwise surface flow, and deeper in TNB beneath the strong TNB polynya (Kurtz & Bromwich, 1985). Formed by persistent offshore winds that remove sea ice as fast as it forms, and often protected by upstream glacial ice barriers, coastal polynyas harbor vertical circulations resembling inverted chimneys, from which "clouds" of dense seawater are dispersed deep below the sea surface. Spreading of the resulting HSSW has been modeled for the TNB and Ross Sea Polynyas (Jendersie et al., 2018). Similar rates of salinity change from 1995 to 2018 in these frequently sampled regions were slightly lower than longer-term declines due to the sharp increase after 2014. All regressions are roughly parallel, as at other sites on the western shelf (Castagno et al., 2019). Averaged "standard level" data (Table S1 in Supporting Information S1) from the surface through 500 m [RI (0–500 m)] show the deep trend is also representative of the full summer water column. In the shallower Hayes Bank vicinity [HB (400 m)] the trend picks up a recent salinity increase to its east in Little America Basin (LAB), where a stronger rate change may reflect freshening CS inflow from the westward slope (Thompson et al., 2018) and coastal currents.

Salinity increases westward on the Ross CS from relatively fresh inflows in the east and stronger sea ice production in coastal polynyas to the west. Most sea ice formed in situ or imported onto the CS will be removed by persistent southerly winds (Figure 1), leaving only a small fraction behind for melting. Summer precipitation is roughly balanced by evaporation (Porter et al., 2019), but salinity decreases during that season of minimal sea ice production. The long-term trend in Figure 2 is equivalent to 2.45 m more FW in a 500 m water column in 2020 than in 1957. Near RI, that rise corresponds to adding ~0.6 m of FW/month during DJF relative to 500 m salinities, increasing more rapidly below than above 200 m (Figure S1 in Supporting Information S1). From 1976–1977 to 2006–2007, however, the salinity on five sections along the RIS decreased more rapidly above 200 m, as might be expected from summer ice front attrition and melting into the coastal current. The inverse

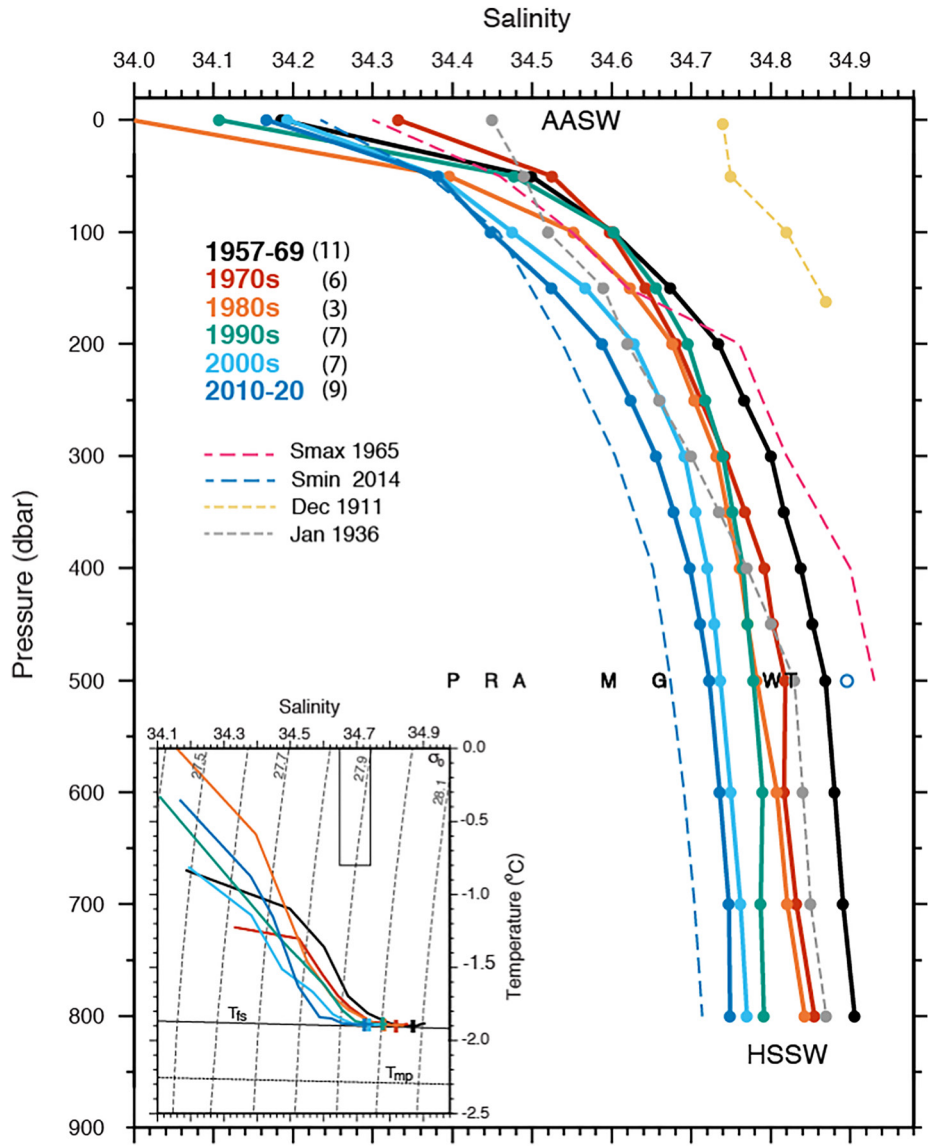

Figure 3. Salinity/depth and temperature/salinity profiles near Ross Island (RI). Solid lines link decadal averages at 50 and 100 dbar intervals (Table S1 in Supporting Information S1); dashed lines show years with the highest and lowest 500 m salinities from 1957 to 2020, plus 1936 and 1911. Profiles from the early 1990s through 2001 crossed 500 dbar at the lettered salinities near Pine Island, eastern Ross, Amery, Mertz, southern George VI, and Western Ronne shelf ice, and in Terra Nova Bay. An open blue circle marks the equivalent absolute salinity for 2010–2020 near RI. On the T/S insert with isopycnal anomaly background, tics locate 500 dbar values from the main figure along the surface freezing temperature line (T_{fs}). The effect of pressure at 500 dbar on the in situ melting point of ice is shown by the T_{mp} line, also from Fofonoff and Millard (1983). A black rectangle approximates the Antarctic Bottom Water domain in Figure 8.

situation near RI could result from northward branching of part of that current. Sea ice formation and seawater supply changes that influence salinity near RI are addressed below.

3.2. Regional Winds and Sea Ice Production

HSSW on the western Ross CS is strongly influenced by the brine released as sea ice is formed in and seaward of wind-driven coastal polynyas (Martin et al., 2007; Petty et al., 2014). Annual restoring of the HSSW reservoir requires sufficient winter brine release to balance summer freshening (Figure S1 in Supporting Information S1), year-round glacial ice melting and relatively low salinity inflows. A 20 km^3/yr increase in sea ice area export across a fluxgate near the CS break from 1992 to 2008 implied a salinity increase of 0.0023/yr to its south

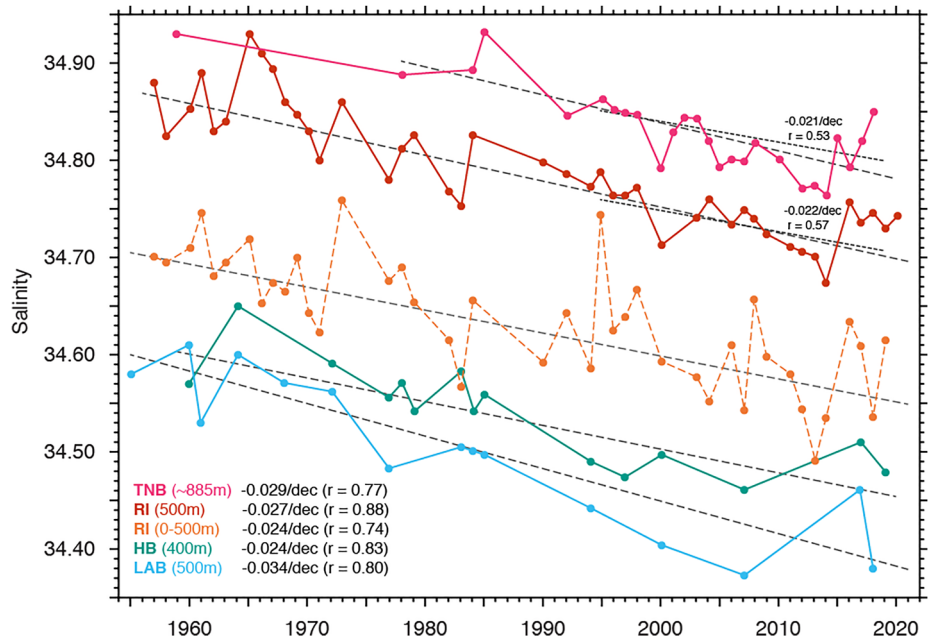

Figure 4. Freshening over 6.3 decades at four coastal areas on the Ross Sea continental shelf (Figure 1). Dashed linear regressions for Terra Nova Bay (TNB) are from 850 to 900 m within the area 74.83–75.3°S and 163.4–166.0°E. For the RI area, (500 m) as in Figure 2, plus (0–500 m) averages. Hayes Bank (400 m) data are near the Ross Ice Shelf (RIS), ~172–175°W. Little America Basin (LAB) (500 m) salinities are also near the RIS, ~160.3–165.9°W. Dotted rates cover 1995–2018 for the TNB and RI areas (Castagno et al., 2019).

(Comiso et al., 2011), roughly equal and opposite the salinity decline over that period (Figure 2). Ice export over the latter years of that study was similar to a 2013 estimate (Tian et al., 2020), but a more recent sea ice export estimate was more variable than trending (Silvano et al., 2020). Annual ice area export has typically been around a third of winter maximum extent in the larger Ross Sea sector, 130°W-160°E (Comiso, 2010; Petty et al., 2014; Tamura et al., 2016), and grew faster in the 1992–2008 interval than from 1979 to 2018 (Parkinson, 2019). The few measurements of exported ice salinity suggest a brine release of ~30 kg from each m^3 of seawater frozen over the CS, but sea ice thickness varies widely near the shelf break (Kurtz & Markus, 2012; Maksym & Jeffries, 1996; Tian et al., 2020). Understanding the sea ice role in freshening is further complicated by high import variability, 20%–60% of ice export. Low import onto the eastern shelf enables stronger on-shelf production, in turn accounting for the recent HSSW rebound (Comiso et al., 2011; Silvano et al., 2020). By that measure, weakening northward winds over the eastern shelf likely damped ice production east of ~170°W, while being more than offset by the stronger northward tendency over the larger central and western shelf (Figure 1).

Southern Ocean sea ice extent increases since 1979 have been largest in the Ross sector and, while not strongly dependent on export from the CS, are generally attributed to strengthening winds (Holland & Kwok, 2012; Parkinson, 2019). The NCEP2 reanalysis winds often used in regional studies (Comiso et al., 2011; Dinniman et al., 2018; Kanamitsu et al., 2002) are stronger than the higher resolution ERA5 winds that more closely track coastal measurements from 1980 to 2018 (Dong et al., 2020), albeit with Ross area observations limited to the western CS. While not well constrained before 1979, the ERA5 extension back to 1950 (Bell et al., 2020) shows strongly meridional surface winds over the western and central CS, trending more NNE than the means (Figure 1). Average wind speed over the full record increased by 0.05 m/s/dec during the March-November sea ice season from 1956 to 2019 (Figure 5). Assuming stronger southerly winds increased sea ice formation on the CS, its impact on freshening would have depended on whether the exported ice was also thinner or saltier, and accompanied by more snow blown into more leads. Although the generally NE directional tendency may have enhanced export by reducing congestion and ridging in the NW sector (Figure 1), the "sea ice season" lengthened by more than a month over the CS from 1979 to 2015 (Ackley et al., 2020). Rising air temperature on RI, ~0.25°/dec since 1957, still averages well below freezing in summer, as along the RIS (Jacobs & Giulivi, 1998; Turner et al., 2004). Given the sea ice thickness and salinity caveats above, stronger brine release over the full CS could

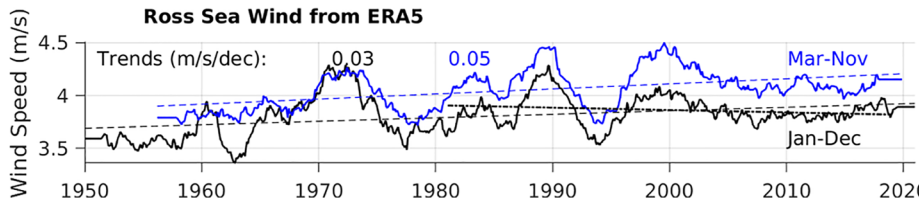

Figure 5. Time series of monthly 10 m wind speed averaged over the Ross Sea continental shelf from an ERA5 reanalysis (Bell et al., 2020), with linear regressions. Continuous lines show time series smoothed with 3-year moving window averaging, using all available data (black), and only winter (Mar-Nov, blue), the latter for 1956–2019 (Figure 1). Without the extension prior to 1979, the full year trend would be weakly negative over the last 4 decades (Hersbach et al., 2019).

have limited freshening, with the March-November wind fluctuations in Figure 5 contributing to Figure 2 salinity variability. Brine release would first need to have balanced increasing summer water column stratification, marked by salinity (density anomaly) changes of −0.103 (−0.09)/dec in the upper 200 m along the RIS from 1976–1977 to 2006–2007, versus −0.028 (−0.078)/dec at depth (Figure 4). Overcoming that seasonal stratification would have required ∼15 kg more brine/dec, equivalent to an 0.5 m/dec growth in sea ice production under strengthening winter winds (Figure 5).

3.3. Antarctic Surface Water and Ice Shelf Melting

AASW forms during brief summers on the Ross CS, freshened by precipitation and melting, and heated by sunlight on open water under prevailing southerly winds (Bromwich et al., 1992). Studies have suggested future RIS vulnerability to AASW incursions near RI (Reese et al., 2018; Tinto et al., 2019), where the local circulation can advect seasonally warmed surface water beneath relatively thin shelf ice into the RIS cavity (Stewart et al., 2019). Ekman and Coriolis effects on the coastal current could drive cavity inflow, as shown in modeling studies (Jendersie et al., 2018; Mack et al., 2019). Surface mixed layer depths, following Holte and Talley (2009), averaged 115 ± 28 m with no significant trend on five summer transects along the RIS calving front from 1976–1977 to 2006–2007. Most all were shallower than the ice front draft (Figure 6), and profiles were close enough to the ice (350 ± 170 m in early February 2007) to record melt-driven staircase structures within the "mixed" layers. Summer salinities in the upper 200 m along the calving front declined over the same period (Section 3.2), while increasing from east to west (not shown), consistent with the underlying isohalines and influence of saltier-westward shelf waters being upwelled by persistent offshore winds. The upper water column is cooled to the surface freezing temperature (Figure S2 in Supporting Information S1) for most of the year, however, and salinized by sea ice formation and deep mixing in coastal leads and polynyas. Late summer warm inflows near 225 m beneath the outer RIS have led to proposed mechanisms for drawing shallow AASW into the ice cavity, including subduction below a wedge-shaped coastal current (Arzeno et al., 2014; Malyarenko et al., 2019; Stewart et al., 2019). Melting near the calving front is much higher than the overall RIS basal average (Horgan et al., 2011), but without evidence that attrition has risen over the last several decades, AASW driven basal melting is unlikely to have contributed substantially to RSF.

3.4. Modified Circumpolar Deep Water and Ice Shelf Melting

Identified by a "warm" Circumpolar Deep Water component formed by mixing over the continental slope, MCDW has typically occupied a broad density band between the Antarctic Surface and Shelf Waters (Orsi & Wiederwohl, 2009; Whitworth et al., 1998). It intrudes farthest onto the Ross CS where the slope front current encounters a bathymetric depression near the shelf break (Hayes & Davey, 1975; St-Laurent et al., 2013). Identified by mid-depth temperature maxima, lower dissolved oxygen and less depleted oxygen isotope values, inflows move southward toward the RIS cavity along or across a saddle in a N-S submarine ridge (Hayes Bank, Figure 6). Often depicted as a continuous sheet or tongue (Countryman & Gsell, 1966; Jacobs & Giulivi, 2010), the intermittent appearance and spatial variability of MCDW in year-round drifter data on the outer CS (Porter et al., 2019) indicate that eddies are likely the more common mode of inflow and transport. Modeling has also shown eddy concentrations near RI and the RIS front, some moving both to and from the ice shelf cavity (Mack et al., 2019; Stewart & Thompson, 2015). Return flow from beneath the RIS west of HB in 1984 (Figure 6) was consistent with cavity access being restricted to the outer, thinner shelf ice. That figure also suggests MCDW eddies moving

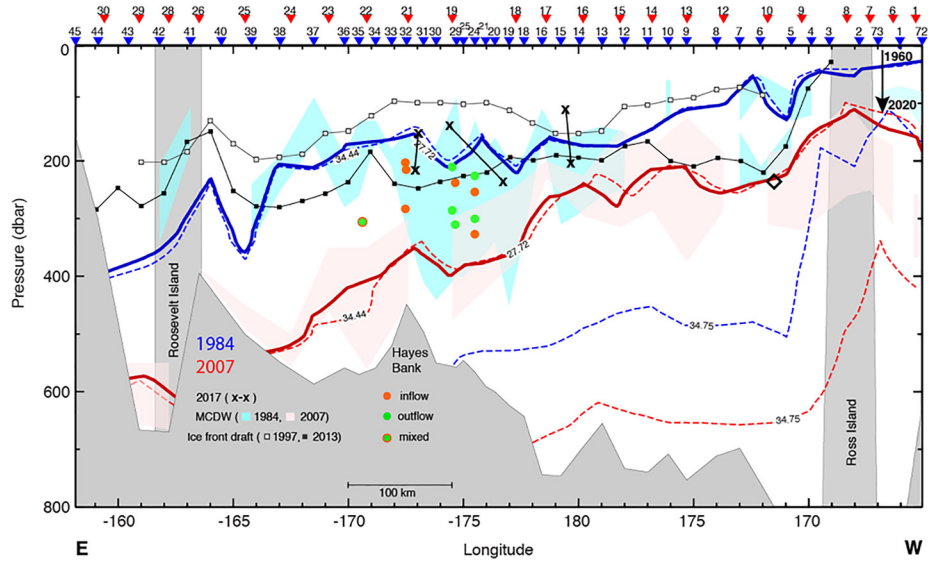

Figure 6. Seawater salinity and density from summer profiles near the Ross Ice Shelf in 1983–1984, 2006–2007, and 2016–2017 (**x-x**), the latter from Porter et al. (2019). Shaded Modified Circumpolar Deep Water depth ranges, defined by temperature maxima and dissolved oxygen minima, typically bracket the 34.44 isohaline, closely tracked by the 27.72 isopycnal (1027.72 kg/m^3). The upper right arrow represents a six-decade isohaline deepening near Ross Island (RI). Colored dots show the positions and 1984 average N-S flow directions from bottom-moored instruments (Oregon State University Buoy Group, 1989). An open black diamond at 229 dbar east of RI locates a nearby sub-ice shelf mooring (Arzeno et al., 2014). Ice front drafts were estimated from ship in 1997 and BEDMAP data in 2013 (Fretwell et al., 2013; Keys et al., 1998). Bathymetry is from the 1984 stations, with subsurface projections of the Roosevelt and Ross Island surface positions.

westward along the RIS front, thus able to fuel seasonally warmer cavity inflow near RI (Jendersie et al., 2018; Tinto et al., 2019). Weak MCDW signals east of HB have appeared at multiple depths in the meandering LAB circulation (Figure 1, Porter et al., 2019). Slight dissolved oxygen minima near bottom in 2007 (not shown) were at temperatures close to year-round measurements near Roosevelt Island in 1957–1958 (Crary, 1961).

The westward shoaling isohalines and RIS calving front drafts in Figure 6 align with seasonal MCDW and AASW influence on ice thickness in that direction (Arzeno et al., 2014; Stewart et al., 2019), abetted by constrained ice flow and fracturing around RI (Reese et al., 2018). The overall shallower ice front draft in 1997 may have resulted from a few decades of basal melting prior to large calving events around 2000 (Keys et al., 1998; Lazzara et al., 1999; Martin et al., 2007), although major calving was not reported west of Roosevelt Island prior to its thicker front in 2013. MCDW was generally more than 100 m deeper in 2007 than 1984, adding some protection from winter cooling, but being farther from southward-deepening basal ice would have allowed mixing over a longer path to weaken its melting potential. MCDW might also be seen as an example of oceanic heat "trapped" below modeled surface FW "lenses" from glacial ice melt, making it available for enhanced ice shelf melting (Golledge et al., 2019). The existence of FW lenses is questionable on the Ross CS, however, as meltwater is quickly mixed into seawater and summer vertical stratification is more than balanced by winter cooling and brine release, helping to erode MCDW in the process. As in other regions with large cold-water ice shelves, much of the RIS meltwater is contained in outflows of "ice shelf water" at temperatures below the surface freezing point and levels near outer-shelf sill depths (Jacobs et al., 1970).

Moorings near HB and the RIS in 1983–1984 (Figure 6) showed both year-round MCDW persistence and winter cooling at depths of 210–327 m (Jacobs & Giulivi, 1998), with seasonal cycling from 0.3 to 1.0°C above the in situ melting point (Figure S2 in Supporting Information S1). MCDW was warmer than the overlying AASW on six sections along the full RIS front over four decades, even in summer (same figure), an indication that it has been more effective than AASW at outer ice shelf melting. Cavity penetration is limited by the RIS draft, also reflected in net outflow at several sites (dots in Figure 6), with the re-circulated residual heat then becoming available for ice shelf melting downstream. Other than one late summer month, annual average MCDW temperatures in 1983–1984 were warmer than recorded in a multi-year 225 m record under the RIS near RI (Arzeno et al., 2014).

Deeper and cooler in 2007 than in 1984, MCDW was closer to 1984 depths directly north of the coastal current in 2016–2017 drifter data (Porter et al., 2019). Those shallower depths may result from the drifters being farther from the ice shelf, prior to any subduction beneath the coastal current. Questions remain about the effect of freshening on inflow strength and frequency (Dinniman et al., 2018; Silvano et al., 2018), but the "warm" MCDW has likely played a lesser role in overall RIS basal melting than the deeper, colder HSSW evaluated below.

3.5. High Salinity Shelf Water and Ice Shelf Melting

HSSW dominates the RIS cavity circulation, with temperatures near the sea surface freezing point (MacAyeal, 1984). Its greater density and depth provide access to basal ice and grounding lines well beyond the reach of AASW & MCDW, leveraging thermal forcing by the effect of pressure on the in situ melting point of ice (Figure 3 inset). Over the full record its 500 m salinity decline of 0.17 was accompanied by a temperature rise of only 0.013°C, with ~3/4 of that rise from the influence of lower salinity on the in situ freezing point. That temperature change is an order of magnitude less than 700–1100 m Southern Ocean warming between the 1950s and 1980s (Gille, 2002). The Ross CS system thus appears relatively stable, even as the HSSW salinity trend is on track to drop below 34.6 by the 5050s (Figure 2). Some models predict much higher temperatures on circumpolar continental shelves by 2100 (Bronselaer et al., 2018; Purich & England, 2021), including replacement of shelf waters by warm deep water from north of the CS in the Weddell Sea (Daae et al., 2020; Hellmer et al., 2017). The Ross and Weddell CS domains are similar in area, shelf waters and ice shelves, but estimates of imbalance melting and freezing have differed substantially over time, with large uncertainties (e.g., Adusumilli et al., 2020; Rignot et al., 2013). Freshening could alter the open shelf and ice cavity circulations, as depicted in Weddell modeling with atmospheric CO_2 rising by 1%/yr (Naughten et al., 2021). In that simulation a sea ice induced salinity decrease ~50 years into the future is similar to observed salinity change on the Ross CS over the past half century. Perhaps their modeled basal mass loss under the Filchner-Ronne, little changed over a longer period, implies little change over coming decades in basal melting of the RIS.

3.6. Ross Ice Shelf Mass Balance

About half of the Ross Sea CS is covered by the giant RIS, mostly exposed at depth to seawater near the freezing point, and warmer during brief summers near its calving front. In the mid-2000s net basal melting occurred only under the East Antarctic Ice Sheet (EAIS) sourced western RIS (Rignot et al., 2013). Shelf waters initially gain access to the basal ice at melting point temperatures that rise by ~0.075°/100 dbar (Figure 3), enhancing erosion of the thicker ice near deep glacier ungrounding lines. Melting freshens and cools the seawater, increasing its buoyancy and leading to basal freezing, an "ice pump" (Lewis & Perkin, 1986) that returns salt to the water column while enhancing cavity circulation and inflow. From a simple box model using summer chlorofluorocarbon and thermohaline data near the RIS, basal melting appeared higher in 1984 than 1994 and 2000 (Smethie & Jacobs, 2005), while the isopycnal slopes in Figure 6 suggest a stronger sub-ice shelf circulation and melting in 2007 than in 1984. Shelf waters along the RIS have freshened at similar rates (Figure 4), indicating that corresponding density changes along the calving front would have caused little change in the baroclinic cavity circulation strength. That is consistent with similar dynamic height differences relative to 500 m between ocean stations near each end of the RIS front on several E-W sections, 10–15 cm higher at the eastern end, with nearly equal height increases of ~20 cm above that depth from 1970 to 2020 (not shown). For comparison, satellite-derived sea surface height changes from 1992 to 2011, with global, regional and enhanced Antarctic shelf sea components (Rye et al., 2014), would be 22 cm if linearly expanded from 1970 to 2020. That study attributed a sharp southward increase in Ross sea level to the halosteric influence of meltwater from upstream, with little influence from the RIS. Meltwater from grounded ice streams can spike during jokulhlaups (e.g., Carter & Fricker, 2012; Stearns et al., 2008), but such outflows are intermittent and not known to have risen over recent decades.

Significant ocean driven change in RIS basal melt rates has seemed unlikely from the minor salinity induced HSSW warming (Figure 2), consistent with minimal near-bottom temperature change along the calving front on repeat sections from 1968 to 1994 (Jacobs & Giulivi, 1998), or from 1957 to 1958 to 2006–2007, as noted above. Observational [modeling] estimates of RIS basal melting over 5 [2.5] decades through 2014 varied widely and now appear generally high, averaging 64 ± 24 Gt/yr (n = 11) [102 ± 38 Gt/yr; n = 8], after excluding a few outliers and normalizing to an ice shelf area of 500,000 km^2. Both exceed the 47.7 Gt/yr (~10 cm/yr) obtained from a 2003-2008 mass balance study (Rignot et al., 2013), in turn close to the 50 ± 64 Gt/yr from a Lagrangian

analysis of ICESat data (Moholdt et al., 2014) and a model result of ~9 cm/yr (Jendersie et al., 2018). Some early studies may not have reported net melt, covered the full ice cavity, or adjusted for the limited range of higher melting within a few tens of km of the calving front (Horgan et al., 2011). A re-survey of 1973 thickness estimates confirmed relative RIS stability over recent decades, finding an insignificant 3.7 ± 4.8 m (~9 ± 11 cm) thinning over 42 years (Das et al., 2020), consistent with the slight observed warming during that period, ~0.01°C at 500 m in Figure 2. Little change may have occurred in the ice shelf firn layer or spreading rate, although tributary ice streams slowed from 2003 to 2009 (Campbell et al., 2017). The resulting regionally thinner shelf ice could have increased basal freezing by allowing seawater, cooled by melting at greater depths, to rise higher in the water column. Alternatively, if the 3.7 m of RIS thinning above were only from basal melting, it would have added ~0.4 Gt/yr of FW to the Ross CS regime, close to a 0.3 Gt/yr mass imbalance during from 2003 to 2008, i.e., 7.8 Gt/yr net EAIS side melting minus 7.5 Gt/yr net WAIS side freezing (Rignot et al., 2013). Uncertainties are high, with the Ross WAIS side ±20 Gt/yr in that study and ±68 Gt/yr from 1994 to 2018 in Adusumilli et al. (2020). Accounting for RSF from added glacial meltwater also requires a growing increase between actual and balanced ice melting, which is difficult to wring from local sources.

3.7. Freshening by Imbalance Glacial Ice Melting Upstream

Meltwater generated east of the Ross Sea will freshen seawater that flows westward in the coastal and slope currents. With high circumpolar ice shelf melt rates directly upstream in the Amundsen Sea, the large volume of FW generated there has been assumed and modeled to account for observed and modeled salinity changes in the Ross Sea (Castagno et al., 2019; Jacobs & Giulivi, 2010; Nakayama et al., 2020). Quantifying such inferences over the 2003–2008 ICESat period (Rignot et al., 2013), imbalance basal melting (actual minus steady-state, $B\text{-}B_{ss}$) for 18 upstream ice shelves from 72 to 157°W was 196 Gt/yr, with B-Bss 27% of B. Over longer periods others have reported 123 Gt/yr from 2003 to 2018 for ice shelves in the WAIS and west Antarctic Peninsula drainage basins 20–24 (Smith et al., 2020), and 162 Gt/yr from 1994 to 2018 for 16 of the ice shelves above (Adusumilli et al., 2020). Methods can differ, some equating melting with ice shelf thinning or missing parts of the large ice shelves, while uncertainties can exceed imbalances, and regional forcing variability can be high (Dutrieux et al., 2014; Paolo et al., 2018). Nonetheless, ice shelf melting and thinning drives most grounded ice sheet loss (Pritchard et al., 2012), increasing glacier velocity and downstream calving. Smaller ice sheet discharges in the same upstream region (Rignot et al., 2019), not included in the earlier ICESat estimate, raise the 2003–2008 imbalance melting to 275 Gt/yr.

The long-term near linear salinity declines on the Ross CS (Figure 4) suggest a similarly increasing rate of FW availability from upstream sources. While evidence for recent glacier change in Amundsen sector dates from the 1940s (Smith et al., 2017), satellite observations enabling rate estimates began after the 1960s, a time when there was no clear 500 m salinity trend near RI (Figure 2). From that information and the timing of Pine Island Glacier ungrounding (Jenkins et al., 2010), we assume imbalanced ice shelf basal melting in that region began around 1970, implying a growth of ~72 Gt/dec (Figure 7a) to reach the above 275 Gt/yr in 2008. An earlier start date would result in a smaller rate of change, and the lower upstream meltwater estimates (circle and box in Figure 7a) yield increases of 63 and 42 Gt/dec. The 72 Gt/dec rate may be biased high by relatively strong Pacific sector meltwater flux during the ICESat period (Adusumilli et al., 2020). It extrapolates to a mass loss rate consistent with the modeled freshening on the Ross CS (Dinniman et al., 2018), but smaller imbalances exceed downstream FW demand (next paragraph). An oxygen isotope based estimate of meltwater inventory in the SE Amundsen Sea suggests an increase of 0.037 m/yr over an 800-m water column from 1994 to 2020 (Hennig et al., in prep). That is similar to the 0–500 m demand near RI (0.039 m/yr, assuming isohaline end of winter salt balance), and would be augmented by the larger combined imbalance FW releases from southwest Amundsen ice shelves, 1994–2018 (Adusumilli et al., 2020). Ice stream acceleration and ice front retreat upstream of the Ross Sea (MacGregor et al., 2012; Mouginot et al., 2014) also point to an increasing production of icebergs, portions of which will melt during westward transport. Meltwater derived from the imbalance between actual and steady state iceberg calving over the same upstream region has been estimated as 160 Gt/yr from 2005 to 2011 (Liu et al., 2015). The combined basal melting and calving, equivalent to an ~114 Gt/dec increase in potentially available FW, can be compared with the amount needed to freshen the Ross Sea CS.

FW flux onto the open Ross CS can be estimated from its seawater volume (~225,000 km^3), rate of salinity change and an inflow compatible with residence time estimates. We assume Figure 4 coastal freshening applies

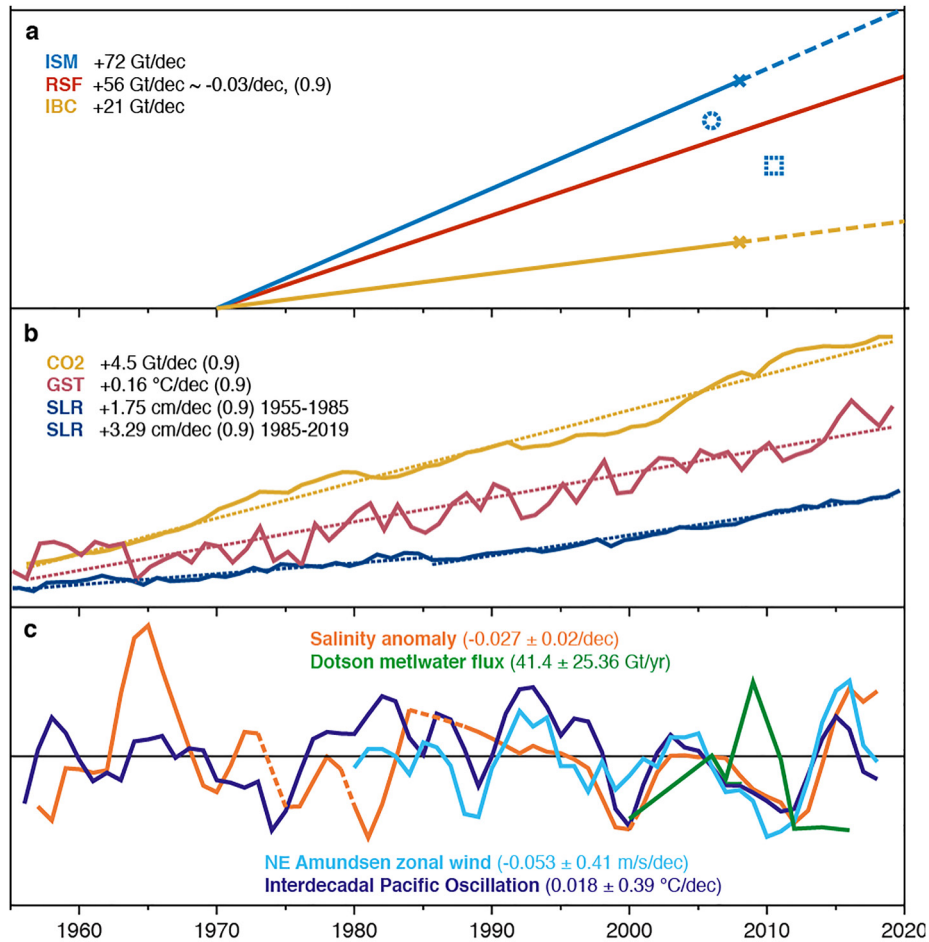

Figure 7. Trends, variability and correlation coefficients for Ross Sea Freshening (RSF) and related local, regional and global parameters. (a) RSF = Ross CS freshwater increase for a salinity change of −0.03/dec and residence time of 3.6 years; ISM and IBC = imbalance ice shelf melting and 0.5 iceberg calving in the upstream Amundsen & Bellingshausen Seas (Liu et al., 2015; Rignot et al., 2013, 2019); The blue circle and square are ice shelf melt rates derived from Adusumilli et al. (2020) and Smith et al. (2020). (b) CO_2 = global carbon dioxide emissions (Ritchie & Roser, 2020); GST = global surface temperature (Lenssen et al., 2019); SLR = global sea level rise (Church & White, 2011, extended). (c) Parameter trends and Dotson Ice Shelf average melting with standard deviations of plotted variability. Two-year running average salinity from Figure 2; Dotson melt from Jenkins et al. (2018); winds (70.2–71.8°S, 102–115°W) from Holland et al. (2019); IPO tripole index from Henley et al. (2015). Relatable to GST and the IPO, but not plotted: Ross Island air temperature, 1957–2015, +0.23°C/dec (0.4), Turner et al. (2004), and the Southern Annular Mode, 1957–2019, +0.5/dec (0.5), Marshall (2003).

throughout the CS and is represented at all depths by the ~0.03/dec change at 500 m (Figure 2). A 200 km^2 fluxgate extending northward from Cape Colbeck (~158°W) and westward along the eastern shelf break encompasses the coastal current and intermittent intrusions or eddies from or across the slope current. A seawater inflow of 2 Sv (2 million m^3/s) at a mean velocity of 1.16 cm/s then corresponds to a 3.6-year residence time on the CS, within the range inferred from geochemical tracers and below 4.1–7.5 year estimates for the windless RIS cavity (Loose et al., 2009; Trumbore et al., 1991). That implies a FW inflow increase of ~56 Gt/dec, similar to modeled inflow volumes and ranges of salinity change (Assmann & Timmermann, 2005; Kusahara & Hasumi, 2014; Nakayama et al., 2020). Melting along the RIS calving front could add up to 10 Gt/y of FW to the coastal current if it eroded as much as 50 m/yr (Porter et al., 2019), less than 10% its advance rate, but without any evidence for long-term change in ice front melting. FW is also exported from the CS as sea ice, ~500–600 km^3/yr from 1992 to 2018 (Comiso et al., 2011; Silvano et al., 2018), comparable to the upstream 538 ± 94 km^3/yr ice shelf balance melting midway during that period (Rignot et al., 2013). The imbalance FW supply increase of 114 Gt/dec is double the Ross CS demand (Figure 7a, where the full basal melting and half the iceberg calving component are plotted separately). The difference between meltwater supply and downstream demand would have been available

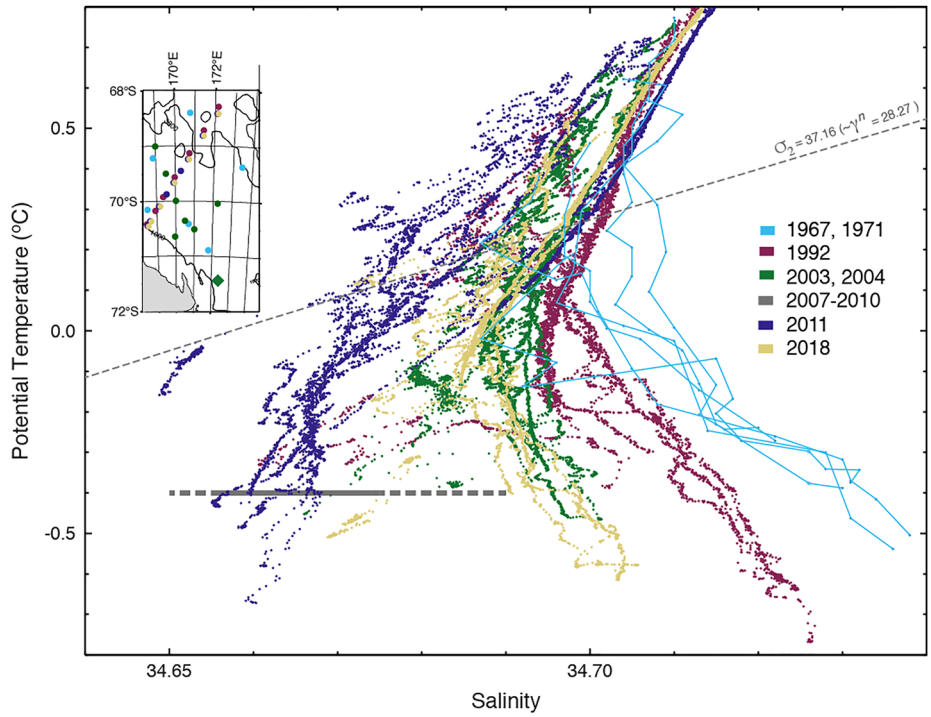

Figure 8. Temperature/Salinity variability over 5 decades in and above Antarctic Bottom Water (AABW) northwest of the Ross Sea. Unsmoothed profiles are from CTD and earlier bottle data from 1050 to 3,400 m at sites on the inset station map, with 1992, 2011 and 2018 from the western end of the SO4P repeat ocean section. Solid (dashed) gray lines along −0.4° show the range of summer (year round) monthly average salinities near 1890 m, ∼40 m above bottom, 2007–2010 (Gordon et al., 2015) on the upstream continental slope (green diamond south of 71°S). The 37.16 isopycnal anomaly (∼28.27 kg/m^3 neutral density) defines the upper AABW boundary (Whitworth et al., 1998).

to account for icebergs that melt elsewhere, offset brine drainage increase from stronger sea ice formation and export, and freshen off-shelf components of the Southern Ocean circulation.

3.8. Freshening Seaward of the Ross Continental Shelf

Seawater exported from the Ross CS moves westward near the coastline, off-shelf near the surface and into the abyssal ocean after mixing with off-shelf waters along and across the Antarctic Slope Front. Over several decades, the resulting deep outflows have led to freshening AABW near the western end of the SO4P repeat ocean section (Figure 8) and downstream to the west (Aoki et al., 2020; Jacobs & Giulivi, 2010; Shimada et al., 2012). By 2011, bottom salinities there were lower than in the overlying deep water, unusual for waters sourced from the western Ross CS, a trend that had reversed by 2018 in response to saltier shelf water after ∼2014 (Castagno et al., 2019; Silvano et al., 2020). Most profiles also display low-salinity, low-temperature near isopycnal intrusions in and above the AABW, similar to continental slope plumes in the northwest Ross Sea (Gordon et al., 2004), and reminiscent of a 1971 feature tracked nearby over a wide area seaward of the continental slope (Carmack & Killworth, 1978). Such intrusions would be expected to shoal as freshening shelf water and its mixing products become insufficiently dense to form AABW defined by neutral densities >28.27 kg/m^3. However, continental slope and rise subsets of the 1992–2011–2018 repeat section in Figure 8 show vertically averaged salinity changes of −0.005/dec in the AABW versus −0.003/dec in the overlying CDW, with the latter integration reaching up to 600 m, a typical regional CS break depth. That is consistent with a greater CFC-11 inventory in AABW than lower CDW from early mid 1990s sections in the Pacific-Indian sector (Orsi et al., 2002). Larger changes near 140°E imply continued freshening downstream, in accord with 2–3 decade changes over a broader region (Aoki et al., 2013; Kobayashi, 2018; Purkey et al., 2019).

Figure 2 salinity variability includes several short periods of equal or greater rates of change, including one starting in 2007 that tracks stronger ice shelf melting upstream (Jenkins et al., 2018). Near bottom salinities

downstream of the Ross CS and upstream of the SO4P section (Figure 8) declined by 0.007/yr over the same period, faster than the long-term CS rate. That change has been attributed to strengthening NCEP easterlies forcing the slope front and HSSW southward on the CS, in turn providing overlying lower salinity shelf water access to the continental slope mixing region (Gordon et al., 2015). Such effects may occur, but the Figure 2 salinity decline was steeper for several years after 2007, ERA5 reanalysis winds are weaker than the lower-resolution NCEP product (Section 3.2), and the prevailing southerlies have trended more northeastward over the west-central shelf break (Figure 1). Seasonal to decadal fluctuations in winds (Figure 5), sea ice cover and HSSW reservoir volume will add variability to abyssal properties downstream. From ~1969 to 2011, however, the coldest bottom water in Figure 8 freshened in parallel with the HSSW, and since 1995 the near-bottom T/S gradients project to shelf water temperatures at salinities close to measured values near the northern ends of CS troughs (Castagno et al., 2019). With near-bottom SO4P salinity tracking Figure 2 HSSW fluctuations, bottom water freshening has likely resumed since its uptick in 2018. Subject to such reversals, a forward projection of the 1969–2011 salinity change near −0.5°C in Figure 8 indicates classically defined AABW production in the NW Ross Sea could end in the 2050s.

4. Summary and Discussion

This compilation of a robust set of HSSW thermohaline properties in the southwest Ross Sea is based on data from 43 austral summers from 1956 to 1957 through 2019–2020, the longest ocean record near Antarctica. Its −0.027/dec salinity trend at 500 m extends a similar prior result using fewer selected profiles over a smaller area through 2008 (Jacobs & Giulivi, 2010). The freshening there is representative of other Ross CS locations (Figure 4), indicating that future regional salinity change can continue to be monitored at readily accessible sites near RI or TNB (Figure 1). Both the trend and its short-term variability have propagated into deeper abyssal regions north of the CS, as shown in Figure 8, probably increasing salinity differences between the Pacific and Indian-Atlantic basins of the Southern Ocean (Boyer et al., 2005). The melting potential of an associated HSSW warming of 0.013°C is mostly offset by the impact of lower salinity on the freezing point. With little reported evidence for changing precipitation minus evaporation on the Ross CS, moderate wind strengthening from an extended ERA5 reanalysis may have enhanced sea ice production and export, reducing if not counteracting (Haumann et al., 2016) the salinity decline. The giant RIS has added little to the freshening, given a relatively small imbalance between glacier inflow and surface accumulation versus calving, basal melting and freezing, with slight measured thinning over four decades. Basal melting near deep RIS ungrounding lines is more sensitive to the in situ melting point dependence on pressure than to freshening HSSW (Figure 3 inset). Fluctuating MCDW inflows (Figure 6) that extend beneath the outer ice shelf are likely to melt more glacial ice than the seasonal AASW (Figure S2 in Supporting Information S1).

An accounting of upstream imbalance glacial ice melting and calving confirms prior conjecture that increasing ice shelf meltwater release in the Amundsen & Bellingshausen Seas has been the proximate cause of RSF. Salinity at 500 m near RI reached a record minimum in 2014, then rose by 0.083 in 2016 (Figure 2), part of a rebound attributed to wind induced changes in sea ice imported to the Ross CS (Silvano et al., 2020). The short-term salinity variability is also relatable to the Interdecadal Pacific Oscillation, and to zonal winds over the CS break and ice shelf melting in the Amundsen Sea (Figure 7c). That forcing influences mCDW access to the regional glacial ice (Holland et al., 2019), including the Amundsen's representative Dotson Ice Shelf (Jenkins et al., 2018), in turn leading to fluctuating salinities downstream near RI. If the past RSF trend continues, HSSW defined by temperatures near the surface freezing point and salinities above ~34.6 will disappear at 500 m near RI in the 2050s, and somewhat later from the full CS, assuming saltier conditions prevail at greater depths in TNB (Figure 4). The declining salinity of HSSW freshened downstream AABW from ~1970 to 2011, followed by a reversal in 2018 (Figure 8). The associated temperatures there are more variable than trending, unlike the broader scale warming in deep ocean basins near Antarctica (Purkey et al., 2019). Without more persistent reversals, the bottom water in this region could drop below its defining density by the 2050s.

Growing sea ice extent in the larger Ross sector may have been a response to stronger winds around a deepening Amundsen Sea Low (Raphael et al., 2016). While that feature is centered well north of the Ross CS near the western end of its annual east-west migration, regional ice extent would have been enhanced by more on-shelf sea ice production and export under stronger offshore winds (Figure 1). Observations of exported sea ice volume and salt content are insufficient to quantify its influence on RSF, but the variably stronger wind forcing, +9%

over 6 decades (March-November in Figure 5), could have also increased ocean circulation strength on the Ross CS, resulting in a shorter residence time for salinizing shelf waters. Modeling of the shelf circulation with a 20% increase in wind forcing (Dinniman et al., 2018) yielded a weaker MCDW inflow with added freshening. Modeling of the analogous Weddell Sea regime (Daae et al., 2020; Hellmer et al., 2017; Naughten et al., 2021) also predicted freshening, mainly from sea ice changes, with much stronger CO_2 forcing enhancing warm water access to the Filchner-Ronne ice shelf cavities during the next century. A continuation of glacial ice loss upstream of the Ross Sea will lengthen its CS records of salinity change and rising FW content, and resume AABW freshening downstream.

Deep salinity change along the Ross Sea coastline has been remarkably linear over more than 6 decades (Figure 4). While linear growth rates of upstream melting and calving are also depicted in Figure 7a, the rates of ice sheet discharge began to increase after ~2000 and accelerated in the last of four decades from 1979 to 2017 (Rignot et al., 2019). Melting has a quadratic response to ocean temperature, but a linear dependence on ocean velocity and pressure (Fofonoff & Millard, 1983; Holland et al., 2008; MacAyeal, 1984). A linear response would fit higher melting from a stronger ocean circulation with relatively little temperature change (Jacobs et al., 2011). Ice shelf thinning and melting estimates are also subject to method and timing, one example being the large, meltwater productive Getz Ice Shelf directly upstream of the Ross CS. From ocean data near its several ice fronts, average basal melting of 1.1 m/yr in the cold summer of 1999–2000 increased to 4.1 m/yr in the warmer 2006–2007 (Jacobs et al., 2013) when Getz was contributing a third of the regional meltwater imbalance. The earlier result is comparable to a satellite derived thinning of 1.76 m/yr over two decades (Christie et al., 2018); the latter is closer to the 4.2–4.3 m/y from 2003 to 2008 (Rignot et al., 2013) and 1994–2018 (Adusumilli et al., 2020). Over longer intervals, regional and global change records and indices can appear or be projected as nearly linear (Figures 7a and 7b; Levermann et al., 2020; Joughin et al., 2021), with the RI air temperature increase both exceeding the global average and including intervals of opposite trends (Bertler et al., 2004). Global sea level rise (SLR) also appears nearly linear over several decades in Figure 7b, but has accelerated since ~1985, and more recently (Rye et al., 2014). With the ice sheets as major contributors, that change could become even more exponential in the future (Church & White, 2011; Oppenheimer & Glavovic, 2019; Rignot et al., 2011).

In flagging the risk that rising fossil fuel consumption poses to the WAIS, Mercer (1978) postulated that atmospheric CO_2 concentration would double in ~50 years. As that timeline nears, emissions have doubled, the CO_2 level has risen by a fourth (Friedlingstein et al., 2020) and parts of the WAIS have displayed a growing mass imbalance (The IMBIE team, 2018). Mercer's proxy for the beginning of deglaciation was rising air temperature at calving fronts, but ice shelf vulnerability to ocean warming was also noted, and Doake (1976) cited for the depth dependence of its melting point. That is one reason ice shelves exist, as CS waters cooled to the surface freezing point by sea ice formation are then deeply overturned, gaining an ice melting potential of 0.075°C/100 dbar (Figure 3 inset; T_{mp} vs. T_{fs}). Stronger basal melting at higher pressures is abetted by deep ungrounding lines and the density/tidal/melt-freeze driven ice cavity circulations. Although strong ice shelf basal melting upstream of the Ross Sea has been known for decades (Jacobs et al., 1996; Potter & Paren, 1985), more than 70% of that melting and iceberg calving balances glacier inflow and surface accumulation (Rignot et al., 2013). The remaining imbalance may result less from a warming sea than from changing atmospheric and oceanic circulations over the last half-century (Holland et al., 2019; Jacobs et al., 2011). As ice shelves thin and lose traction with the seafloor, faster glacier inflows and steady freshening raise sea level. A modeled "abrupt jump" in the pace of Antarctic ice loss resulted from forcing scenarios consistent with Paris Climate Agreement policies that allow 3°C of global warming (DeConto et al., 2021). SLR and other climatic impacts could spur divisive geo-engineering projects with high risk/benefit ratios (Robock, 2020). Of course wars and pandemics could restrict population growth and its impacts, greater atmospheric moisture transport could increase snowfall on the WAIS, and large ice shelves could continue to benefit from weak MCDW incursions. Without substantial energy source mitigation by homo "sapiens," however, glacial ice vulnerability to continued erosion by air-sea-ice responses to our business-as-usual "lifestyles" seems very likely to drown the world's beaches and other shorelines.

Data Availability Statement

The data in Figures 1–3 and S1 in Supporting Information S1 are from various archives and publications, summarized as summer average "standard depth" measurements in Table S1 in Supporting Information S1 and its references (https://doi.org/10.15784/601458). Salinities underlying the RSF record are supplemented by interpolated

annual values and associated temperatures in Table S2 in Supporting Information S1 and the equivalent meltwater increase on the Ross CS in Figure 7a. The Hayes Bank and LAB comparisons in Figure 4 are from bottle and CTD measurements archived at the National Oceanographic Data Center, National Centers for Environmental Information (NODC/NCEI). Data for Figures 5–7 were compiled from ERA5 reanalyses and other sources noted in their captions. Figure 8 observations are from the SO4P repeat section in 1992, 2011 & 2018, available from cchdo.ucsd.edu, and from Eltanin 1967, 1971, AnSlope 2003, 2004 and CALM 2007–2010 projects, as reported to NODC. The 2-year temperature record in Figure S2 in Supporting Information S1 is from 1983–1984 moorings (Oregon State University Buoy Group, 1989), with the upper water column information from summer sections along the RIS in 1968 (*Eltanin*), 1976 (*Northwind*), 1984 and 1994 (*Polar Sea*) and 2000 and 2007 (*NB Palmer*), logged at NODC and Integrated Earth Data Applications (IEDA). We would welcome summer observations near Ross Island (Figure 1) in years that would fill data gaps or extend the record length (Figure 2, Table S2 in Supporting Information S1).

Acknowledgments
We thank the agencies and individuals who have financed, acquired, processed, reported or provided the data used in this study. Investigators and other personnel associated with the support of numerous ships, ice platforms and drifting floats were also essential in obtaining the existing observations. We have benefitted from anonymous and editorial reviews, and from assistance and discussions with the late T. Amos and J. Ardai, and with G. Budillon, R. Dunbar, R. Guerrero, R. Locarnini, F. Nitsche, S. O'Hara, D. Porter, N. Robinson, W. Smethie, S. Stammerjohn, C. Stewart and X. Yuan. The authors declare no financial conflicts of interest in this work, which was supported by the NSF (OPP-1644159), TIAA, SSA and NASA (80NSSC20K1158).

References

Ackley, S., Stammerjohn, S., Maksym, T., Smith, M., Cassano, J., Guest, P., et al. (2020). Sea-ice production and air/ice/ocean/biogeochemistry interactions in the Ross Sea during the PIPERS 2017 autumn field campaign. *Annals of Glaciology*, *61*, 181–195. https://doi.org/10.1017/aog.2020.31

Adusumilli, S., Fricker, H., Medley, B., Padman, L., & Siegfried, M. (2020). Interannual variations in meltwater input to the Southern Ocean from Antarctic ice shelves. *Nature Geoscience*, *13*, 616–620. https://doi.org/10.1038/s41561-020-0616-z

Aoki, S., Kitade, Y., Shimada, K., Ohshima, K., Tamura, T., Bajish, C., et al. (2013). Widespread freshening in the seasonal ice zone near 140°E off the Adelie Land coast, Antarctica, from 1994 to 2012. *Journal of Geophysical Research: Oceans*, *118*(11), 6046–6063. https://doi.org/10.1002/2013JC009009

Aoki, S., Yamazaki, K., Hirano, D., Katsumata, K., Shimada, K., Kitade, Y., et al. (2020). Reversal of freshening trend of Antarctic bottom water in the Australian-Antarctic basin during 2010s. *Nature Scientific Reports*, *10*, 14415. https://doi.org/10.1038/s41598-020-71290-6

Arzeno, I., Beardsley, R., Limeburner, R., Owens, B., Padman, L., Springer, S., et al. (2014). Ocean variability contributing to basal melt rate near the ice front of Ross Ice Shelf, Antarctica. *Journal of Geophysical Research*, *119*(7), 4214–4233. https://doi.org/10.1002/2014JC009792

Assmann, K., & Timmermann, R. (2005). Variability of dense water formation in the Ross Sea. *Ocean Dynamics*, *55*, 68–87. https://doi.org/10.1007/s10236-004-0106-7

Bell, B., Hersbach, H., Berrisford, P., Dahlgren, P., Horányi, A., Muñoz Sabater, J., et al. (2020). ERA5 monthly averaged data on pressure levels from 1950 to 1978 (preliminary version). *Copernicus Climate Change Service Climate Data Store*. Retrieved from https://cds.climate.copernicus.eu/cdsapp#!/dataset/reanalysis-era5-pressure-levels-monthly-means-preliminary-back-extension?tab=overview

Bertler, N., Barrett, P., Mayewski, P., Fogt, R., Kreutz, K., & Shulmeister, J. (2004). El Nino suppresses Antarctic warming. *Geophysical Research Letters*, *31*, L15207. https://doi.org/10.1029/2004GL020749

Boyer, T., Levitus, S., Antonov, J., Locarnini, R., & Garcia, H. (2005). Linear trends in salinity for the world ocean, 1955–1998. *Geophysical Research Letters*, *32*, L01604. https://doi.org/10.1029/2004GL021791

Bromwich, D., Carrasco, J., & Stearns, C. (1992). Satellite observations of katabatic-wind propagation for great distances across the Ross Ice Shelf. *Monthly Weather Review*, *120*(9), 1940–1949. https://doi.org/10.1175/1520-0493(1992)120<1940:SOOKWP>2.0.CO;2

Bromwich, D., Nicolas, J., & Monaghan, A. (2011). An assessment of precipitation changes over Antarctica and the Southern Ocean since 1989 in contemporary global reanalyses. *Journal of Climate*, *24*, 4189–4209. https://doi.org/10.1175/2011jcli4074.1

Bronselaer, B., Winton, M., Griffies, S., Hurlin, W., Rodgers, K., Sergienko, O., et al. (2018). Change in future climate due to Antarctic meltwater. *Nature*, *564*, 53–58. https://doi.org/10.1038/s41586-018-0712-z

Campbell, A., Hulbe, C., & Lee, C.-K. (2017). Ice stream slowdown will drive long-term thinning of the Ross Ice Shelf, with or without ocean warming. *Geophysical Research Letters*, *45*(1), 201–206. https://doi.org/10.1002/2017GL075794

Carmack, E. (1977). Water characteristics of the Southern Ocean south of the polar front. In M. Angel (Ed.), *A voyage of discovery, G. Deacon 70th anniversary volume, supplement to Deep-Sea Research* (pp. 15–41). Pergamon Press.

Carmack, E., & Killworth, P. (1978). Formation and interleaving of abyssal water masses off Wilkes Land, Antarctica. *Deep-Sea Research*, *25*, 357–369. https://doi.org/10.1016/0146-6291(78)90563-5

Carter, S., & Fricker, H. (2012). The supply of subglacial meltwater to the grounding line of the Siple Coast, West Antarctica. *Annals of Glaciology*, *53*(60), 267–280. https://doi.org/10.3189/2012AoG60A119

Castagno, P., Capozzi, V., DiTullio, G., Falco, P., Fusco, G., Rintoul, S., et al. (2019). Rebound of shelf water salinity in the Ross Sea. *Nature Communications*, *10*, 5441. https://doi.org/10.1038/s41467-019-13083-8

Christie, F., Bingham, R., Gourmelon, N., Steig, E., Bisset, R., Pritchard, H., et al. (2018). Glacier change along West Antarctica's Marie Byrd Land sector and links to inter-decadal atmosphere-ocean variability. *The Cryosphere*, *12*(7), 2461–2479. https://doi.org/10.5194/tc-12-2461-2018

Church, J., & White, N. (2011). Sea-level rise from the late 19th to the early 21st century. *Surveys in Geophysics*, *32*, 585–602. https://doi.org/10.1007/s10712-011-9119-1

Comiso, J. (2010). *Polar Oceans from space*. (pp. XIV+507). Springer-Verlag NY. https://doi.org/10.1007/978-0-387-68300-3

Comiso, J., Kwok, R., Martin, S., & Gordon, A. (2011). Variability and trends in sea ice extent and ice production in the Ross Sea. *Journal of Geophysical Research*, *116*, C04021. https://doi.org/10.1029/2010jc006391

Countryman, K., & Gsell, W. (1966). *Operations Deep Freeze 63 and 64, Summer oceanographic features of the Ross Sea* (Technical Report 190, p. 193). U. S. Naval Oceanographic Office. https://doi.org/10.5962/bhl.title.46747

Crary, A. (1961). Glaciological studies at little America station, Antarctica, 1957 and 1958. In *International Geophysical Year glaciological report 6, IGY World Data Center A: Glaciology*. American Geographical Society.

Daae, K., Hattermann, T., Darelius, E., Mueller, R., Naughten, K., Timmermann, R., & Hellmer, H. (2020). Necessary conditions for warm inflow toward the Filchner Ice Shelf, Weddell Sea. *Geophysical Research Letters*, *47*(22), e2020GL089237. https://doi.org/10.1029/2020GL089237

Das, I., Padman, L., Bell, R., Fricker, H., Tinto, K., Hulbe, C., et al. (2020). Multi-decadal basal melt rates and structure of the Ross Ice Shelf, Antarctica, using airborne ice penetrating radar. *Journal of Geophysical Research: Earth Surface*, *125*(3), e2019JF005241. https://doi.org/10.1029/2019JF005241

Deacon, G. (1975). The oceanographical observations of Scott's last expedition. *Polar Record*, *17*(109), 391–396. Scott Polar Research Institute 53792. https://doi.org/10.1017/S0032247400032265

DeConto, R., Pollard, D., Alley, R., Velicogna, I., Gasson, E., Gomez, N., et al. (2021). The Paris Climate Agreement and future sea-level rise from Antarctica. *Nature*, *593*, 83–89. https://doi.org/10.1038/s41586-021-03427-0

Dinniman, M., Klinck, J., Hofmann, E., & Smith, W. (2018). Effects of projected changes in wind, atmospheric temperature, and freshwater inflow on the Ross Sea. *Journal of Climate*, *31*(4), 1619–1635. https://doi.org/10.1175/JCLI-D-17-0351.1

Doake, C. (1976). Thermodynamics of the interaction between ice shelves and the sea. *Polar Record*, *18*(112), 37–41. https://doi.org/10.1017/S0032247400028692

Dong, X., Wang, Y., Hou, S., Ding, M., Yin, B., & Zhang, Y. (2020). Robustness of the recent global atmospheric reanalyses for Antarctic near-surface wind speed climatology. *Journal of Climate*, *33*(10), 4027–4043. https://doi.org/10.1175/JCLI-D-19-0648.1

Dutrieux, P., De Rydt, J., Jenkins, A., Holland, P., Ha, H., Lee, S., et al. (2014). Strong sensitivity of Pine Island ice-shelf melting to climatic variability. *Science*, *343*, 174–178. https://doi.org/10.1126/science.1244341

Fofonoff, N., & Millard, R. (1983). Algorithms for computation of fundamental properties of seawater. *UNESCO Technical Papers in Marine Science*, *44*, 53. http://ioc-unesco.org/

Fretwell, P., Pritchard, H., Vaughan, D., Bamber, J., Barrand, N., Bell, R., et al. (2013). Bedmap2: Improved ice bed, surface and thickness datasets for Antarctica. *The Cryosphere*, *7*, 375–393. https://doi.org/10.5194/tc-7-375-2013

Friedlingstein, P., O'Sullivan, M., Jones, M., Andrew, R., Hauck, J., Olsen, A., et al. (2020). Global carbon budget 2020. *Earth System Science Data*, *12*, 3269–3340. https://doi.org/10.5194/essd-12-3269-2020

Friedrich, R., & Schlosser, P. (2013). Data report stable isotope analysis: NBP0702, version 1.0. *Interdisciplinary Earth Data Alliance*. https://doi.org/10.1594/IEDA/100272

Gill, A. (1973). Circulation and bottom water production in the Weddell Sea. *Deep-Sea Research*, *20*(2), 111–140. https://doi.org/10.1016/0011-7471(73)90048-X

Gille, S. (2002). Warming of the Southern Ocean since the 1950s. *Science*, *295*(5558), 1275–1277. https://doi.org/10.1126/science.1065863

Golledge, N., Keller, E., Gomez, N., Naughten, K., Bernales, J., Trusel, L., & Edwards, T. (2019). Global environmental consequences of twenty-first-century ice-sheet melt. *Nature*, *566*, 65–72. https://doi.org/10.1038/s41586-019-0889-9

Gordon, A., Huber, B., & Busecke, J. (2015). Bottom water export from the western Ross Sea, 2007 through 2010. *Geophysical Research Letters*, *42*, 5387–5394. https://doi.org/10.1002/2015GL064457

Gordon, A., Zambianchi, E., Orsi, A., Visbeck, M., Giulivi, C., Whitworth, T., & Spezie, T. (2004). Energetic plumes over the western Ross Sea continental slope. *Geophysical Research Letters*, *31*(21), L21302. https://doi.org/10.1029/2004GL020785

Haumann, A., Gruber, N., Munnich, M., Frenger, I., & Kern, S. (2016). Sea-ice transport driving Southern Ocean salinity and its recent trends. *Nature*, *537*, 89–92. https://doi.org/10.1038/nature19101

Hayes, D., & Davey, F. (1975). *A geophysical study of the Ross Sea, Antarctica* (Vol. 28). *Initial Reports of the Deep Sea Drilling Project*. https://doi.org/10.2973/dsdp.proc.28.134.1975

Hellmer, H., Kauker, F., Timmermann, R., & Hattermann, T. (2017). The fate of the southern Weddell Sea continental shelf in a warming climate. *Journal of Climate*, *30*(12), 4337–4350. https://doi.org/10.1175/JCLI-D-16-0420.1

Henley, B., Gergis, J., Karoly, D., Power, S., Kennedy, J., & Folland, C. (2015). A tripole index for the interdecadal Pacific oscillation. *Climate Dynamics*, *45*(11–12), 3077–3090. https://doi.org/10.1007/s00382-015-2525-1

Hersbach, H., Bell, B., Berrisford, P., Biavati, G., Horányi, A., Muñoz Sabater, J., et al. (2019). ERA5 monthly averaged data on pressure levels from 1979 to present. *Copernicus Climate Change Service Climate Data Store*. https://doi.org/10.24381/cds.6860a573

Holland, P., Bracegirdle, T., Dutrieux, P., Jenkins, A., & Steig, E. (2019). West Antarctic ice loss influenced by internal climate variability and anthropogenic forcing. *Nature Geoscience*, *12*, 718–724. https://doi.org/10.1038/s41561-019-0420-9

Holland, P., Jenkins, A., & Holland, D. (2008). The response of ice shelf basal melting to variations in ocean temperature. *Journal of Climate*, *21*, 2558–2572. https://doi.org/10.1175/2007JCLI1909.1

Holland, P., & Kwok, R. (2012). Wind-driven trends in Antarctic sea-ice drift. *Nature Geoscience*, *5*, 872–875. https://doi.org/10.1038/ngeo1627

Holte, J., & Talley, L. (2009). A new Algorithm for finding mixed layer depths with Applications to Argo data and subantarctic mode water formation. *Journal of Atmospheric and Oceanic Technology*, *26*(9), 1920–1939. https://doi.org/10.1175/2009JTECHO543.1

Horgan, H., Walker, R., Anandakrishnan, S., & Alley, R. (2011). Surface elevation changes at the front of the Ross Ice Shelf: Implications for basal melting. *Journal of Geophysical Research*, *116*, C02005. https://doi.org/10.1029/2010JC006192

Jacobs, S., Amos, A., & Bruchhausen, P. (1970). Ross Sea oceanography and Antarctic bottom water formation. *Deep-Sea Research and Oceanographic Abstracts*, *17*(6), 935–962. https://doi.org/10.1016/0011-7471(70)90046-X

Jacobs, S., & Giulivi, C. (1998). Interannual ocean and sea ice variability in the Ross Sea. In S. Jacobs & R. Weiss (Eds.), *Ocean, Ice and Atmosphere: Interactions at the Antarctic Continental Margin*. *Antarctic Research Series* (Vol. 75, pp. 135–150). American Geophysical Union. https://doi.org/10.1029/AR075p0135

Jacobs, S., & Giulivi, C. (2010). Large multidecadal salinity trends near the Pacific-Antarctic continental margin. *Journal of Climate*, *23*, 4508–4524. https://doi.org/10.1175/2010JCLI3284.1

Jacobs, S., Giulivi, C., Dutrieux, P., Rignot, E., Nitsche, F., & Mouginot, J. (2013). Getz Ice Shelf melting response to changes in ocean forcing. *Journal of Geophysical Research: Oceans*, *118*(9), 4152–4168. https://doi.org/10.1002/jgrc.20298

Jacobs, S., Giulivi, C., & Mele, P. (2002). Freshening of the Ross Sea during the late 20th century. *Science*, *297*(5580), 386–389. https://doi.org/10.1126/science.1069574

Jacobs, S., Hellmer, H., & Jenkins, A. (1996). Antarctic ice sheet melting in the southeast Pacific. *Geophysical Research Letters*, *23*(9), 957–960. https://doi.org/10.1029/96GL00723

Jacobs, S., Jenkins, A., Giulivi, C., & Dutrieux, P. (2011). Stronger ocean circulation and increased melting under Pine Island Glacier ice shelf. *Nature Geoscience*, *4*, 519–523. https://doi.org/10.1038/ngeo1188

Janout, M., Hellmer, H., Hattermann, T., Huhn, O., Sultenfuss, J., Osterhus, S., et al. (2021). FRIS revisited in 2018: On the circulation and water masses at the Filchner and Ronne ice shelves in the Southern Weddell Sea. *Journal of Geophysical Research: Oceans*, *126*, e2021JC017269. https://doi.org/10.1029/2021JC017269

Jendersie, S., Williams, M., Langhorne, P., & Robertson, R. (2018). The density-driven winter intensification of the Ross Sea circulation. *Journal of Geophysical Research: Oceans*, *123*(11), 7702–7724. https://doi.org/10.1029/2018JC013965

Jenkins, A., Dutrieux, P., Jacobs, S., McPhail, S., Perrett, J., Webb, A., & White, D. (2010). Observations beneath Pine Island Glacier in West Antarctica and implications for its retreat. *Nature Geoscience*, *3*, 468–472. https://doi.org/10.1038/ngeo890

Jenkins, A., Shoosmith, D., Dutrieux, P., Jacobs, S., Kim, T.-W., Lee, S.-H., et al. (2018). West Antarctic Ice Sheet retreat in the Amundsen Sea driven by decadal oceanic variability. *Nature Geoscience*, *11*, 733–738. https://doi.org/10.1038/s41561-018-0207-4

Joughin, I., Shapero, D., Dutrieux, P., & Smith, B. (2021). Ocean-induced melt volume directly paces ice loss from Pine Island Glacier. *Science Advances*, *7*(43), eabi5738. https://doi.org/10.1126/sciadv.abi5738

Kanamitsu, M., Ebisuzaki, W., Woollen, J., Yang, S.-K., Hnilo, J., Fiorino, M., & Potter, G. (2002). NCEP-DOE AMIP-II reanalysis (R-2): 1631-1643. *Bulletin of the American Meteorological Society*, *83*(11), 1631–1644. https://doi.org/10.1175/BAMS-83-11-1631

Keys, H., Jacobs, S., & Brigham, L. (1998). Continued northward expansion of the Ross Ice Shelf, Antarctica. *Annals of Glaciology*, *27*, 93–98. https://doi.org/10.3189/1998AoG27-1-93-98

Kobayashi, T. (2018). Rapid volume reduction in Antarctic bottom water off the Adelie/George V Land coast observed by deep floats. *Deep-Sea Research I*, *140*, 95–117. https://doi.org/10.1016/j.dsr.2018.07.014

Kurtz, D., & Bromwich, D. (1985). A recurring, atmospherically forced polynya in Terra Nova Bay. In *Antarctic Research Series* (Vol. 43, pp. 177–201). American Geophysical Union. https://agupubs.onlinelibrary.wiley.com/doi/abs/10.1029/AR043p0177

Kurtz, D., & Markus, T. (2012). Satellite observations of Antarctic sea ice thickness and volume. *Journal of Geophysical Research*, *117*(C8), C08025. https://doi.org/10.1029/2012JC008141

Kusahara, K., & Hasumi, H. (2014). Pathways of basal meltwater from Antarctic ice shelves. *Journal of Geophysical Research: Oceans*, *119*(9), 5690–5704. https://doi.org/10.1002/2014JC009915

Lazzara, M., Jezek, K., Scambos, T., MacAyeal, D., & van der Veen, C. (1999). On the recent calving of icebergs from the Ross Ice Shelf. *Polar Geography*, *23*(3), 201–212. https://doi.org/10.1080/10889379909377676

Lenssen, N., Schmidt, G., Hansen, J., Menne, M., Persin, A., Ruedy, R., & Zyss, D. (2019). Improvements in the GISTEMP uncertainty model. *Journal of Geophysical Research: Atmospheres*, *124*(12), 6307–6326. https://doi.org/10.1029/2018JD029522

Levermann, A., Winkelmann, R., Albrecht, T., Goelzer, H., Golledge, N., Greve, R., et al. (2020). Projecting Antarctica's contribution to future sea level rise from basal ice shelf melt using linear response functions of 16 ice sheet models (LARMIP-2). *Earth System Dynamics*, *11*, 35–76. https://doi.org/10.5194/esd-11-35-2020

Lewis, E., & Perkin, R. (1986). Ice pumps and their rates. *Journal of Geophysical Research*, *91*(C10), 11756–11762. https://doi.org/10.1029/JC091iC10p11756

Liu, Y., Moore, J., Cheng, X., Gladstone, R., Bassis, J., Liu, H., et al. (2015). Ocean-driven thinning enhances iceberg calving and retreat of Antarctic ice shelves. *Proceedings of the National Academy of Sciences*, *112*(11), 3263–3268. https://doi.org/10.1073/pnas.1415137112

Loose, B., Schlosser, P., Smethie, W., & Jacobs, S. (2009). An optimized estimate of glacial melt from the Ross Ice Shelf using noble gases, stable isotopes, and CFC transient tracers. *Journal of Geophysical Research*, *114*(C8), C08007. https://doi.org/10.1029/2008JC005048

MacAyeal, D. (1984). Thermohaline circulation below the Ross Ice Shelf: A consequence of tidally induced vertical mixing and basal melting. *Journal of Geophysical Research*, *89*(C1), 597–606. https://doi.org/10.1029/JC089iC01p00597

MacGregor, J., Catania, G., Markowski, M., & Andrews, A. (2012). Widespread rifting and retreat of ice-shelf margins in the eastern Amundsen Sea Embayment between 1972 and 2011. *Journal of Glaciology*, *58*, 458–466. https://doi.org/10.3189/2012JoG11J262

Mack, S., Dinniman, M., Klinck, J., McGillicuddy, D., & Padman, L. (2019). Modeling ocean Eddies on Antarctica's cold water continental shelves and their effects on ice shelf basal melting. *Journal of Geophysical Research: Oceans*, *124*, 5067–5084. https://doi.org/10.1029/2018JC014688

Maksym, T., & Jeffries, M. (1996). Bulk salinity characteristics of first-year sea ice in the Pacific sector of the southern oceans. *Antarctic Journal of the U.S.*, *31*(2), 99–101. https://www.nsf.gov/geo/opp/antarct/ajus/nsf9828/9828html/c5.htm

Malyarenko, A., Robinson, N., Williams, M., & Langhorne, P. (2019). A wedge mechanism for summer surface water inflow into the Ross Ice Shelf cavity. *Journal of Geophysical Research: Oceans*, *124*(2), 1196–1214. https://doi.org/10.1029/2018JC014594

Marshall, G. (2003). Trends in the southern annular mode from observations and reanalyses. *Journal of Climate*, *16*(24), 4134–4143. https://doi.org/10.1175/1520-0442(2003)016<4134:titsam>2.0.co;2

Martin, S., Drucker, R., & Kwok, R. (2007). The areas and ice production of the western and central Ross Sea polynyas, 1992-2002, and their relation to the B-15 and C-19 iceberg events of 2000 and 2002. *Journal of Marine Systems*, *68*(1), 201–214. https://doi.org/10.1016/j.jmarsys.2006.11.008

Mercer, J. (1978). West Antarctic ice sheet and CO_2 greenhouse effect: A threat of disaster. *Nature*, *271*, 321–325. https://doi.org/10.1038/271321a0

Moholdt, G., Padman, L., & Fricker, H. (2014). Basal mass budget of Ross and Filchner-Ronne ice shelves, Antarctica, derived from Lagrangian analysis of ICESat altimetry. *Journal of Geophysical Research: Earth Surface*, *119*(11), 2361–2380. https://doi.org/10.1002/2014JF003171

Mouginot, J., Rignot, E., & Scheuchl, B. (2014). Sustained increase in ice discharge from the Amundsen Sea embayment, West Antarctica, from 1973 to 2013. *Geophysical Research Letters*, *41*, 1576–1584. https://doi.org/10.1002/2013GL059069

Munk, W. (2003). Ocean freshening, sea level rising. *Science*, *300*(5628), 2041–2043. https://doi.org/10.1126/science.1085534

Nakayama, Y., Timmermann, R., & Hellmer, H. (2020). Impact of West Antarctic ice shelf melting on Southern Ocean hydrography. *The Cryosphere*, *14*, 2205–2216. https://doi.org/10.5194/tc-14-2205-2020

Naughten, K., De Rydt, J., Rosier, S., Jenkins, A., Holland, P., & Ridley, J. (2021). Two-timescale response of a large Antarctic ice shelf to climate change. *Nature Communications*, *12*, 1991. https://doi.org/10.1038/s41467-021-22259-0

Oppenheimer, M., & Glavovic, B. (2019). Sea Level Rise and Implications for Low-Lying Islands, Coasts and Communities. Chapter 4, Coordinating Lead Authors, et al. *IPCC Special Report on the Ocean and Cryosphere in a Changing Climate*. Retrieved from https://www.ipcc.ch/srocc/download-report/

Oregon State University Buoy Group. (1989). *Deep water archive, Southern Ocean data*, PRISM (Ross Sea) 1984-87. Retrieved from http://cmrecords.net

Orsi, A., Smethie, W., & Bullister, J. (2002). On the total input of Antarctic waters to the deep ocean: A preliminary estimate from chlorofluorocarbon measurements. *Journal of Geophysical Research*, *107*(C8), 3122. https://doi.org/10.1029/2001JC000976

Orsi, A., & Wiederwohl, C. (2009). A recount of Ross Sea waters. *Deep-Sea Research Part II: Topical Studies in Oceanography*, *56*(13–14), 778–795. https://doi.org/10.1016/j.dsr2.2008.10.033

Paolo, F., Padman, L., Fricker, H., Adusumilli, S., Howard, S., & Siegfried, M. (2018). Response of Pacific-sector Antarctic ice shelves to the El Nino/southern oscillation. *Nature Geoscience*, *11*, 121–126. https://doi.org/10.1038/s41561-017-0033-0

Parkinson, C. (2019). A 40-yr record reveals gradual Antarctic sea ice increases followed by decreases at rates far exceeding the rates seen in the Arctic. *Proceedings of the National Academy of Sciences*, *116*(29), 14414–14423. https://doi.org/10.1073/pnas.1906556116

Petty, A., Holland, P., & Feltham, D. (2014). Sea ice and the ocean mixed layer over the Antarctic shelf seas. *The Cryosphere*, *8*(2), 761–783. https://doi.org/10.5194/tc-8-761-2014

Porter, D., Springer, S., Padman, L., Fricker, H., Tinto, K., Riser, S., et al. (2019). Evolution of the seasonal surface mixed layer of the Ross Sea, Antarctica, observed with autonomous profiling floats. *Journal of Geophysical Research: Oceans*, *124*, 4934–4953. https://doi.org/10.1029/2018JC014683

Potter, J., & Paren, J. (1985). Interaction between ice shelf and ocean in George VI Sound, Antarctica. In *Antarctic Research Series* (Vol. 43, pp. 35–58). American Geophysical Union. https://agupubs.onlinelibrary.wiley.com/doi/abs/10.1029/AR043p0035

Pritchard, H., Ligtenberg, S., Fricker, H., Vaughan, D., van den Broeke, M., & Padman, L. (2012). Antarctic ice-sheet loss driven by basal melting of ice shelves. *Nature*, *484*, 502–505. https://doi.org/10.1038/nature10968

Purich, A., & England, M. (2021). Historical and future projected warming of Antarctic shelf bottom water in CMIP6 models. *Geophysical Research Letters*, *48*(10), e2021GL092752. https://doi.org/10.1029/2021GL092752

Purkey, S., & Johnson, G. (2012). Global contraction of Antarctic bottom water between the 1980s and 2000s. *Journal of Climate*, *25*(17), 5830–5844. https://doi.org/10.1175/JCLI-D-11-00612.1

Purkey, S., Johnson, G., Talley, L., Sloyan, B., Wijffels, S., Smethie, W., et al. (2019). Unabated bottom water warming and freshening in the South Pacific Ocean. *Journal of Geophysical Research: Oceans*, *124*(3), 1778–1794. https://doi.org/10.1029/2018JC014775

Raphael, M., Marshall, G., Turner, J., Fogt, R., Schneider, D., Dixon, D., et al. (2016). The Amundsen Sea low: Variability, change, and impact on Antarctic climate. *Bulletin of the American Meteorological Society*, *97*(1), 111–121. https://doi.org/10.1175/BAMS-D-14-00018.1

Reese, R., Gudmundsson, G., Levermann, A., & Winkelmann, R. (2018). The far reach of ice-shelf thinning in Antarctica. *Nature Climate Change*, *8*, 53–57. https://doi.org/10.1038/s41558-017-0020-x

Rignot, E., Jacobs, S., Mouginot, J., & Scheuchl, B. (2013). Ice shelf melting around Antarctica. *Science*, *341*, 266–270. https://doi.org/10.1126/science.1235798

Rignot, E., Mouginot, J., Scheuchl, B., van den Broeke, M., van Wessem, M., & Morlighem, M. (2019). Four decades of Antarctic ice sheet mass balance from 1979-2017. *Proceedings of the National Academy of Sciences*, *116*(4), 1095–1103. https://doi.org/10.1073/pnas.1812883116

Rignot, E., Velicogna, I., van den Broeke, M., Monaghan, A., & Lenaerts, J. (2011). Acceleration of the contribution of the Greenland and Antarctic ice sheets to sea level rise. *Geophysical Research Letters*, *38*, L05503. https://doi.org/10.1029/2011GL046583

Ritchie, H., & Roser, M. (2020). *CO_2 and greenhouse gas emissions*. ourworldindata.org.

Robinson, N., Williams, M., Barrett, P., & Pyne, A. (2010). Observations of flow and ice-ocean interaction beneath the McMurdo Ice Shelf, Antarctica. *Journal of Geophysical Research*, *115*, C03025. https://doi.org/10.1029/2008JC005255

Robock, A. (2020). Benefits and risks of stratospheric solar radiation management for climate intervention (geoengineering). *The Bridge*, Spring 2020, 59–67.

Rye, C., Naveira Garabato, A., Holland, P., Meredith, M., Nurser, A., Hughes, C., et al. (2014). Rapid sea-level rise along the Antarctic margins in response to increased glacial discharge. *Nature Geoscience*, *7*, 732–735. https://doi.org/10.1038/NGEO2230

Shimada, K., Aoki, S., Oshmima, K., & Rintoul, S. (2012). Influence of Ross Sea bottom water changes on the warming and freshening of the Antarctic bottom water in the Australian-Antarctic basin. *Ocean Science*, *8*, 419–432. https://doi.org/10.5194/os-8-419-2012

Silvano, A., Foppert, A., Rintoul, S., Holland, P., Tamura, T., Kimura, N., et al. (2020). Recent recovery of Antarctic bottom water formation in the Ross Sea driven by climate anomalies. *Nature Geoscience*, *13*, 780–786. https://doi.org/10.1038/s41561-020-00655-3

Silvano, A., Rintoul, S., Pena-Molino, B., Hobbs, W., van Wijk, E., Aoki, S., et al. (2018). Freshening by glacial meltwater enhances melting of ice shelves and reduces formation of Antarctic bottom water. *Science Advances*, *4*(4), eeap9467. https://doi.org/10.1126/sciadv.aap9467

Smethie, W., & Jacobs, S. (2005). Circulation and melting under the Ross Ice Shelf: Estimates from evolving CFC, salinity and temperature fields in the Ross Sea. *Deep-Sea Research*, *52*, 959–978. https://doi.org/10.1016/j.dsr.2004.11.016

Smith, B., Fricker, H., Gardner, A., Medley, B., Nilsson, J., & Paolo, F. (2020). Pervasive ice sheet mass loss reflects competing ocean and atmosphere processes. *Science*, *368*(6496), 1239–1242. https://doi.org/10.1126/science.aaz5845

Smith, J., Andersen, T., Shortt, M., Gaffney, A., Truffer, M., Stanton, T., et al. (2017). Sub-ice-shelf sediments record history of twentieth-century retreat of Pine Island Glacier. *Nature*, *541*, 77–80. https://doi.org/10.1038/nature20136

Stearns, L., Smith, B., & Hamilton, G. (2008). Increased flow speed on a large East Antarctic glacier caused by subglacial floods. *Nature Geoscience*, *1*, 827–831. https://doi.org/10.1038/ngeo356

Stewart, A., & Thompson, A. (2015). Eddy-mediated transport of warm circumpolar deep water across the Antarctic shelf break. *Geophysical Research Letters*, *42*, 432–440. https://doi.org/10.1002/2014GL062281

Stewart, C., Christoffersen, P., Nicholls, K., Williams, M., & Dowdeswell, J. (2019). Basal melting of the Ross Ice Shelf from solar heat absorption in an ice-front polynya. *Nature Geoscience*, *12*, 435–440. https://doi.org/10.1038/s41561-019-0356-0

St-Laurent, P., Klinck, J., & Dinniman, M. (2013). On the role of coastal troughs in the circulation of warm circumpolar deep water on Antarctic shelves. *Journal of Physical Oceanography*, *43*(1), 51–64. https://doi.org/10.1175/JPO-D-11-0237.1

Tamura, T., Ohshima, K., Fraser, A., & Williams, G. (2016). Sea ice production variability in Antarctic coastal polynyas. *Journal of Geophysical Research: Oceans*, *121*(5), 2967–2979. https://doi.org/10.1002/2015JC011537

The IMBIE team. (2018). Mass balance of the Antarctic ice sheet from 1992 to 2017. *Nature*, *558*, 219–222. https://doi.org/10.1038/s41586-018-0179-y

Thompson, A., Stewart, A., Spence, P., & Heywood, K. (2018). The Antarctic slope current in a changing climate. *Reviews of Geophysics*, *56*(4), 741–770. https://doi.org/10.1029/2018RG000624

Tian, L., Xie, H., Ackley, S., Tang, J., Mestas-Nunez, A., & Wang, X. (2020). Sea Ice freeboard and thickness in the Ross Sea from airborne (IceBridge 2013) and satellite (ICESat 2003-2008) observations. *Annals of Glaciology*, *61*(82), 24–39. https://doi.org/10.1017/aog.2019.49

Timmermann, R., LeBrocq, A., Deen, T., Domack, E., Dutrieux, P., Galton-Fenzi, B., et al. (2010). A consistent data set of Antarctic ice sheet topography, cavity geometry, and global bathymetry. *Earth System Science Data*, *2*(2), 261–273. https://doi.org/10.5194/essd-2-261-2010

Tinto, K., Padman, L., Siddoway, C., Springer, S., Fricker, H., Das, I., et al. (2019). Ross Ice Shelf response to climate driven by the tectonic imprint on seafloor bathymetry. *Nature Geoscience*, *12*(6), 441–449. https://doi.org/10.1038/s41561-019-0370-2

Trumbore, S., Jacobs, S., & Smethie, W. (1991). Chlorofluorocarbon evidence for rapid ventilation of the Ross Sea. *Deep-Sea Research*, *38*, 845–870. https://doi.org/10.1016/0198-0149(91)90022-8

Turner, J., Colwell, S., Marshall, G., Lachlan-Cope, T., Carleton, A., Jones, P., et al. (2004). The SCAR READER project: Toward a high-quality database of mean Antarctic meteorological observations. *Journal of Climate*, *17*(14), 2890–2898. https://doi.org/10.1175/1520-0442(2004)017<2890:TSRPTA>2.0.CO;2

Whitworth, T., Orsi, A., Kim, S.-J., Nowlin, W., & Locarnini, R. (1998). Water masses and mixing near the Antarctic slope front. In *Antarctic research series* (Vol. 75, pp. 1–27). American Geophysical Union. https://doi.org/10.1029/AR075p0001

References From the Supporting Information

Stevens, C., Hulbe, C., Brewer, M., Stewart, C., Robinson, N., Ohneiser, C., & Jendersie, S. (2020). Ocean mixing and heat transport processes observed under the Ross Ice Shelf control its basal melting. *Proceedings of the National Academy of Sciences*, *117*(29), 16799–16804. https://doi.org/10.1073/pnas.1910760117